SAC1p Is An Integral Membrane Protein That Influences the Cellular Requirement for Phospholipid Transfer Protein Function and Inositol in Yeast

Eric A. Whitters, Ann E. Cleves,* Todd P. McGee, Henry B. Skinner, and Vytas A. Bankaitis

Department of Cell Biology, The University of Alabama at Birmingham, Birmingham, Alabama 35294-0005; and *Department of Microbiology, University of Illinois, Urbana, Illinois 61801

Abstract. Mutations in the *SAC1* gene exhibit allele-specific genetic interactions with yeast actin structural gene defects and effect a bypass of the cellular requirement for the yeast phosphatidylinositol/phosphatidylcholine transfer protein (SEC14p), a protein whose function is essential for sustained Golgi secretory function. We report that SAC1p is an integral membrane protein that localizes to the yeast Golgi complex and to the yeast ER, but does not exhibit a detectable association with the bulk of the yeast F-actin cytoskeleton. The data also indicate that the profound in vivo effects on Golgi secretory function and the organization of the actin cytoskeleton observed in *sac1* mutants result from loss of SAC1p function. This cosuppression of actin and SEC14p defects is a unique feature of *sac1* alleles as mutations in other *SAC* genes that result in a suppression of actin defects do not result in phenotypic suppression of SEC14p defects. Finally, we report that *sac1* mutants also exhibit a specific inositol auxotrophy that is not exhibited by the other *sac* mutant strains. This *sac1*-associated inositol auxotrophy is not manifested by measurable defects in de novo inositol biosynthesis, nor is it the result of some obvious defect in the ability of *sac1* mutants to utilize inositol for phosphatidylinositol biosynthesis. Thus, *sac1* mutants represent a novel class of inositol auxotroph in that these mutants appear to require elevated levels of inositol for growth. On the basis of the collective data, we suggest that SAC1p dysfunction exerts its pleiotropic effects on yeast Golgi function, the organization of the actin cytoskeleton, and the cellular requirement for inositol, through altered metabolism of inositol glycerophospholipids.

THE Golgi complex plays a fundamental role in the regulation of key aspects of intracellular protein and membrane traffic through the eukaryotic secretory pathway. As a result, considerable effort has been directed at the development of powerful biochemical and molecular strategies to identify the factors that govern the secretory functions of this organelle. In *Saccharomyces cerevisiae*, the *SEC14* gene product (SEC14p) is required for secretory protein transport from a late Golgi compartment (Novick et al., 1980; Franzusoff and Schekman, 1989). We have established that SEC14p is a peripheral membrane protein of the yeast Golgi whose function is essential for cell viability and whose structure is highly conserved across significant phylogenetic boundaries (Bankaitis et al., 1989; Cleves et al., 1991*a*, *b*; Salama et al., 1990; H.B. Skinner and V.A. Bankaitis, manuscript in preparation). Moreover, we have demonstrated SEC14p to be the yeast phosphatidylinositol (PI)[1]/phosphatidylcholine (PC) transfer protein (Bankaitis et al., 1990).

To date, the most penetrating insights into the mechanism of SEC14p function have been obtained from a detailed analysis of yeast mutants in which the normally essential cellular requirement for SEC14p is bypassed. It was demonstrated that mutations in any one of at least six genes could effect an efficient bypass of SEC14p, and it was further recognized that such alleles of three of these genes block PC biosynthesis via the CDP-choline pathway (Cleves et al., 1991*b*). On the basis of those data, we proposed that SEC14p functions to establish a critical phospholipid composition in Golgi membranes that is required for Golgi secretory competence. Bypass alleles of the remaining three genes (i.e., *BSD1*, *BSD2*, and *SAC1*) do not block PC synthesis via the CDP-choline pathway, however, and analysis of these genes

E. A. Whitters and A. E. Cleves contributed equally to this study and represent co-first authors.

Dr. Bankaitis' present address is Department of Cell Biology, The University of Alabama at Birmingham, Birmingham, AL 35294-0005.

1. *Abbreviations used in this paper*: BCA, bicinchoninic acid; F-actin, filamentous actin; IP, immunoprecipitation; LSP, low speed pellet; PC, phosphatidylcholine; PI, phosphatidylinositol; PrA, proteinase A; TRSC, Texas red sulfonyl chloride; WC, whole cell.

is expected to yield novel insights into SEC14p function in vivo. One of these genes, *SAC1*, is of singular interest. Not only do *sac1* alleles effect an efficient bypass of the SEC14p requirement, but these same alleles also suppress mutations in *ACT1*, the actin structural gene of yeast, in an allele-specific manner (Cleves et al., 1989; Novick et al., 1989). These findings have identified a previously unanticipated relationship between the organization of the actin cytoskeleton and the function of a Golgi-specific phospholipid transfer protein in vivo, and raise the issue of what role SAC1p plays in this relationship.

In this report, we show that SAC1p is an integral membrane protein that localizes both to the yeast Golgi complex and to the yeast ER, but does not detectably associate with the bulk filamentous actin cytoskeleton in yeast. Moreover, we establish that it is loss of SAC1p function that effects the bypass of SEC14p. Finally, we demonstrate that *sac1* mutations are unique among the other known *sac* mutations in their ability to suppress both *sec14*-associated Golgi defects and defects in actin cytoskeleton function, and that *sac1* alleles are similarly unique in their phenotypic manifestation of a specific inositol auxotrophy in yeast. We offer the general hypothesis that the pleiotropic phenotypes associated with SAC1p dysfunction reflect alterations in some aspect of inositol glycerophospholipid metabolism in *sac1* yeast strains.

Materials and Methods

Strains, Media, and Reagents

Complete genotypes of yeast strains and description of plasmids are listed in Table I. YP, yeast minimal and defined media have been described (Sherman et al., 1983). Yeast minimal media that either lack or contain inositol (1mM) and choline (1mM) were described by Klig et al. (1985). Con A-sepharose, TRITC-conjugated phalloidin, poly-L-lysine, DAPI, indoleacrylic acid, PMSF, chymostatin, pepstatin, leupeptin, sodium pyrophosphate, myo-inositol dehydrogenase, and proteinase K were obtained from Sigma Immunochemicals (St. Louis, MO). The NADH monitoring kit was purchased from LKB-Wallac (Gaithersburg, MD), and NAD was obtained from Boehringer Mannheim Biochemicals (Indianapolis, IN). Protein G-Sepharose was from Pharmacia Fine Chemicals (Piscataway, NJ). Intermediate and secondary antibodies conjugated to fluorochrome were from Jackson ImmunoResearch (West Grove, PA). Reagents for SDS-PAGE were from Bio-Rad Laboratories (Richmond, CA). [^{35}S]-labeled amino acids were purchased under the [^{35}S]Trans-Label trademark (>1,000 Ci/mmol) from ICN Radiochemicals (Irvine, CA). Oxalyticase was from Enzogenetics (Corvallis, OR). Proteinase A antiserum was obtained from E. W. Jones (Carnegie Mellon University, Pittsburgh, PA). The YEp(*KEX2*) plasmid and KEX2p antiserum were obtained from R. Fuller (Stanford University Medical Center, Stanford, CA). Yeast actin antiserum was obtained from D. Drubin (University of California, Berkeley, CA) and B. Haarer (University of Michigan, Ann Arbor, MI).

SAC1p Antibodies

pRE102, a plasmid consisting of a 2.4-kb XbaI *SAC1* minimal complementing fragment subcloned in the vector pTZ18U (Cleves et al., 1989), was

Table I. Yeast Strains

Strain	Genotype	Origin
CTY1-1A*	*MAT a, ura3-52, Δhis3-200, lys2-801, sec14-1*	Bankaitis et al. (1989)
CTY87	*MAT a, ura3-52, sac1-6*	P. Novick
CTY88	*MAT a, ura3-52, sac1-8*	P. Novick
CTY100	*MAT a, ura3-52, Δhis3-200, lys2-801, sec14-1, sac1-26*	Cleves et al. (1989)
CTY150‡	CTY182/pCTY134	Cleves et al. (1989)
CTY182	*MAT a, ura3-52, Δhis3-200, lys2-801*	Bankaitis et al. (1989)
CTY214	*MAT a, ura3-52, ade2-101, leu2-3,112, his4-519, sec14-1*	This study
CTY234‡	CTY182/pCTY136	This study
CTY244	*MAT a, ura3-52, Δhis3-200, lys2-801, sac1-296::HIS3*	Cleves et al. (1989)
CTY402	*MAT a, ura3-52, sac1-7*	P. Novick
CTY403	*MAT α, his4-619, lys2-803, sac1-10*	P. Novick
CTY404	*MAT a, ade2-101, lys2-803, sac1-11*	P. Novick
CTY405	*MAT a, ura3-52, lys2-803, sac1-14*	P. Novick
CTY406	*MAT a, ura3-52, sac1-15*	P. Novick
CTY417	*MATα, ura3, his3, leu2, trp1, ino1-13*	S. Henry
CTY443‡	CTY182/pCTY101	This study
CTY444‡	CTY182/pCTY114	This study
CTY463	*MAT a, ura3-52, Δhis3-200, lys2-801, sac1-102::URA3*	This study
CTY558	*MAT α, ade2-101, ade3, leu2-3,112, Δhis3-200, ura3-52, sec14Δ1::HIS3*/pCTY11	This study
CTY578	*MAT a, ura3-52, Δhis3-200, lys2-801, sec14-1, sac7Δ1::HIS3*	This study
NY226	*MAT a, ura3-52, sac2-1, MOX1*	P. Novick
NY247	*MAT a, ura3-52, sac3-1, MOX1*	P. Novick
AAY1022	*MATa, act1-3, tub2-201, ura3-52, sac6-15*	A. Adams

* The *sec14-1* allele encodes a thermolabile SEC14p whereas all mutant *sac1*, *sac2*, and *sac3* alleles listed in this table result in a *cs* phenotype (Bankaitis et al., 1989; Cleves et al., 1989; Novick et al, 1989).

‡ A detailed description of yeast plasmids pCTY101 and pCTY114 is given in the legend to Fig. 3 *A*. Plasmid pCTY136 is a YEp(*URA3*) vector that carries the yeast *KEX2* gene and causes KEX2p overproduction in the host strain. Plasmid pCTY134 is a YEp(*URA3*) vector that carries an intact *SAC1* gene and causes an approximate 20-fold overproduction of SAC1p in the host strain. Plasmid pCTY11 is a YEp(*LEU2, ADE3*) vector that carries the *SEC14* gene under the control of an attenuated *SEC14* promoter such that this multicopy plasmid sustains the synthesis of SEC14p in yeast at a rate that is very similar to that sustained by the single-copy genomic *SEC14* locus (not shown).

digested with BclI and religated. This resulted in a deletion of the internal 527-bp BclI fragment from the *SAC1* clone. The deletion of the BclI fragment caused a frame shift within the *SAC1* coding sequence such that the unique BclI site was followed by five new codons (the first two of which fortuitously encoded the same amino acids in those positions as the authentic *SAC1* sequence) and a stop codon. The ΔBclI plasmid (pRE138) encodes the first 356 residues of the SAC1p plus three new residues. Using the XhoI site within the *SAC1* gene and the SmaI site in the vector polylinker, a 1.5-kb XhoI-SmaI fragment that encodes SAC1p amino acids 102-356 (plus three new residues) was removed from pRE138 and subcloned into the SalI and HindIII (blunt-ended) polylinker sites of pATH10 (from A. Tzagaloff), an inducible expression vector that contains the promoter, operator, and coding sequence for the *trpE* gene. The resultant plasmid, pRE139, encodes a 593 residue fusion protein representing amino acids 102-356 of the SAC1p (68 kD). *E. coli* strain RR1 (Bolivar et al., 1977) bearing pRE139 produced some 10 mg of fusion protein per liter of cells after an 8-h expression period in tryptophan-free medium supplemented with indoleacrylic acid (20 μg/ml). The hybrid protein was purified via a general procedure for TrpE fusion proteins (Kleid et al., 1981) and found to reside in the supernatant of a 0.1% SDS, 50 mM Tris, pH 7.5, 50 mM EDTA wash of the insoluble fraction of the total cellular lysate. mAbs were generated by standard methods (Kennett, 1980). Balb/C mice were given a primary and two boost injections of 50 μg of fusion protein per injection. Hybridoma cell lines were produced and maintained in the Hybridoma Facility, University of Illinois Biotechnology Center (Urbana, IL). Culture supernatants from the hybridomas were screened for anti-SAC1p antibodies by immunoprecipitation assays of radiolabeled yeast lysates. Two positive clones, hybridoma cell lines C5 and C6, were amplified in cell culture and the anti-SAC1p mAbs were precipitated from culture supernatants by addition of $(NH_4)_2SO_4$ to 50% saturation. For immunoprecipitation (IP) and immunolocalization of SAC1p, a mixture of these two mAbs was used.

Identification of SAC1p

Radiolabeling of yeast with ^{35}S-Trans label and preparation of clarified extracts was performed as described by Bankaitis et al. (1989). Immune complexes were recovered with protein G-Sepharose and sequentially washed twice with IP buffer (50 mM Tris-Cl, pH 7.5, 150 mM NaCl, 0.1 mM EDTA, 0.5% Tween 20), twice with urea wash buffer (2 M urea, 100 mM Tris-Cl, pH 7.5, 200 mM NaCl, 0.5% Tween 20), and twice with 0.1% SDS. Resolution of the immunoprecipitates and autoradiography was performed as described by Schauer et al. (1985). For immunoprecipitations, SAC1p and PrA antibodies were used at final concentrations of 3.3 μg/ml and 8 μg/ml, respectively.

Fractionation of SAC1p

Whole cell (WC), low speed pellet (LSP), 12,000 *g* pellet (P12), 100,000 *g* pellet (P100), and 100,000 *g* supernatant (S100) fractions derived from radiolabeled CTY182 were prepared exactly as described by Bankaitis et al. (1989). Clarified extracts derived from each fraction were treated with PrA and SAC1p antibodies.

Na_2CO_3 Extraction

Strain CTY150 (OD_{600} = 1.0) was radiolabeled for 1 h (100 μCi Trans-label/ml). After termination of radiolabel incorporation by the addition of NaN_3 to 10 mM, the cells were washed twice in 10 mM NaN_3 and then converted to spheroplasts by a 20 min incubation at room temp in 1.4 M sorbitol, 50 mM KPi, pH 7.5, 10 mM NaN_3, 20 μg/ml oxalyticase. The spheroplasts were pelleted gently in a clinical centrifuge and subjected to osmotic lysis by resuspension in 1.0 ml 0.3 M sorbitol, 10 mM MOPS, pH 7.0. Unlysed cells and large debris were removed by centrifugation at 500 *g* for 2 min. Subsequently, 0.5 ml of clarified lysate was removed and saved as the WC fraction. The remaining 0.5 ml was adjusted to 0.1 M Na_2CO_3, pH 11.5, and incubated on ice for 1 h. The sample was then spun at 100,000 g for 1 h yielding the high speed supernatant (S100) and high speed pellet (P100) fractions. The P100 was solubilized in 1% SDS buffer (50 mM Tris, pH 7.5, 1 mM EDTA, 1% SDS). TCA (5% final concentration) was used to precipitate proteins from the WC and S100 fractions, and these precipitates were solubilized in 1% SDS buffer. The WC, S100, and P100 fractions were then diluted in IP buffer and treated with SEC14p antiserum (8 μg/ml final concentration) and SAC1p antibodies.

Immunoprecipitation of SAC1p from sac1^{cs} Mutants

Cultures of wild type and *sac1^{cs}* strains (OD_{600} = 1.0) were radiolabeled for either 1 h or 5 min with [^{35}S]Trans-label (100 μCi/ml). The corresponding extracts were subjected to immunoprecipitation with SEC14p and SAC1p antisera by the regimen described above.

Immunofluorescence

Yeast strains were grown to an early logarithmic stage of growth in complete minimal medium or uracil-deficient medium for plasmid maintenance. Yeast were prepared for immunofluorescence essentially as described by Pringle et al. (1989). Cultures were fixed with 4% formaldehyde (final concentration) first for 15 min in the culture medium and then for 12 h at 4°C in 100 mM potassium phosphate, pH 6.5, 0.5 mM $MgCl_2$ (buffer A). The fixed cells were spheroplasted for 30 min at 37°C in buffer A containing 20 μg/ml oxalyticase followed by four washes in 1× PBS. Washed spheroplasts were placed on poly-L-lysine–coated glass slides and subsequently immersed in methanol (−20°C) for 6 min, and then acetone (−20°C) for 1 min. All incubations and washes were performed at room temp in 1× PBS, 1% BSA. After the final washes, one drop of 1 mg/ml *p*-phenylenediamine (in 90% glycerol, 0.1× PBS) was added to the stained cells which were then sealed under glass coverslips. The samples were photographed using TMAX 400 film (Eastman Kodak Co., Rochester, NY) and a Zeiss axioplan microscope (Carl Zeiss, Inc., Thornwood, NY) equipped for fluorescence with UV filters and an HBO 50-W mercury lamp. Antibody incubations for localization of the SAC1p were: (*a*) anti-SAC1p antibodies (16 μg/ml final concentration), 2 h; (*b*) 15 μg/ml rabbit anti–mouse IgG or sheep anti–mouse IgG, 1 h; and (*c*) 15 μg/ml FITC-conjugated goat anti–rabbit IgG or TRSC-conjugated donkey anti–sheep IgG, 1 h. Antibody incubations for localization of the KEX2p were: (*a*) affinity-purified polyclonal rabbit anti-KEX2p serum (preadsorbed against permeabilized Δ*kex2* spheroplasts, 30 μg/ml final antibody concentration), 2 h; and (*b*) 15 μg/ml FITC-conjugated goat anti–rabbit IgG, 1 h. For the co-localization of actin and the SAC1p, fixed spheroplasts were permeabilized by a 20-min incubation in 1% Triton X-100, 1× PBS, washed four times in PBS, and then placed on polylysine-coated glass slides and allowed to air dry. Actin was visualized using TRITC-conjugated phalloidin (6.6 μM final concentration).

Subcellular Fractionation

Preparation of highly enriched Golgi fractions was performed as described by Cleves et al. (1991*b*) with minor modifications. The sorbitol gradients described in this work were 40–65% for the first gradient and 50–60% for the second gradient. Resolution of the 12,000 *g* pellet fractions, generated by the method of Cleves et al. (1991*b*), was performed by equilibrium flotation in a self-forming 30–55% sucrose gradient essentially as described by Bowser and Novick (1991). 0.5-ml fractions were collected from the top of the gradient and assayed for the appropriate markers.

Construction of a sac7Δ1::URA3 Null Allele

We generated a *sac7Δ1::URA3* allele that is directly analogous to the *sac7::LEU2* null allele previously reported by Dunn and Shortle (1990) to represent an allele-specific suppressor of *act1^{ts}*. Oligonucleotides SAC7-5A (5′CCGAATTCGGTACCAAATTCAACGATTGG-3′) and SAC7-3B (5′CCGCATGCCCCGGTTTATGTAACCACGGG-3′) were used as forward and reverse primers, respectively, to generate an ~1-kb PCR product from a template of yeast genomic DNA. The extreme 5′ end of this PCR product spans the KpnI site that is situated immediately upstream of the *SAC7* gene, and the 3′ end of this product corresponds to the COOH-terminal coding region of *SAC7* (see Dunn and Shortle, 1990). This PCR product was subcloned into a ΔHindIII derivative of pTZ18R as an EcoRI-SphI restriction fragment to yield pRE176. This resultant plasmid was then digested with HincII to release a 480-bp fragment, resulting in a deletion in the plasmid of essentially all of the coding sequence for the minimal SAC7p functional domain (Dunn and Shortle, 1990), the resultant blunt ends were ligated to HindIII linkers, and the yeast *URA3* gene was inserted into that newly created HindIII site to generate the *sac7Δ1::URA3* plasmid pRE180. The disruption allele was excised as a 1.5-kb KpnI-SphI fragment and used to transform strain CTY1-1A to Ura$^+$. The authenticity of the *sac7Δ1::URA3* transformants was confirmed by diagnostic PCR.

Measurement of Intracellular Inositol Pools

The appropriate yeast strains were grown to mid-logarithmic phase (OD_{600} = 1.0–1.2) at 30°C with shaking in the defined minimal media of Klig et al. (1985) supplemented with inositol and choline to a final concentration of 1 mM each (I^+C^+ medium). Cells were harvested by centrifugation, washed four times with the same medium lacking inositol and choline (I^-C^- medium), and resuspended in 3 ml of I^-C^- medium for continued incubation at 30°C with shaking. Samples (1.5 ml) were either removed immediately after resuspension in I^-C^- medium, or 3 h after resuspension, to yield the 0 and 180 min time point samples, respectively. For each sample, cells were pelleted in an Eppendorf tube, resuspended in 50 μl of buffer I (50 mM Tris-HCL, pH 7.4, 20% glycerol, 1 mM EDTA), glass beads (0.2–0.3 mM diam) were added to ~75% of volume, and the tubes were chilled on ice. Each tube was then vortexed ten times in 30-s bursts with a 1-min rest with cooling between bursts. The lysates were clarified by centrifugation for 15 min at 14,000 *g* and supernatants collected for protein and inositol assay.

Inositol was quantitated by a modification of an enzyme-coupled bioluminescence assay developed by Gudermann and Cooper (1986). Briefly, the 80 μl inositol assay cocktail included 50 μl distilled H_2O, 13 μl sodium pyrophosphate (0.1 M, pH 9.0), 8 μl NAD (5 mM), 1.4 μl myo-inositol dehydrogenase (1.5 mU/μl), and 8 μl of either an appropriate dilution of lysate in distilled H_2O (to yield an input of 0.1 μg of protein into the reaction) or a known inositol standard. The reaction was incubated at 25°C for 5 min after which time 80 μl of NADH monitoring reagent, prepared according to the method of Gudermann and Cooper (1986), was added to each assay. Luminescence was monitored immediately, and recorded as a time course over a 5-min period at 20-s intervals using a Lumiphot luminometer. Inositol content of each sample was calculated by determining the initial rates of increase in luminescence vs time, and comparing these rates to those established for samples of known inositol content as described by Gutermann and Cooper (1986). Protein concentrations were determined by the bicinchoninic acid (BCA) assay marketed by Pierce Biochemicals.

Phospholipid Analyses

The appropriate yeast strains were grown to an OD_{600} of ~0.8, total glycerophospholipid was extracted and resolved by two-dimensional paper chromatography exactly as described by Atkinson (1984). Resolved phospholipid species were stained with Rhodamine 6G and visualized under UV light (Christie, 1987). Individual phospholipid species were excised and the lipids extracted from the paper with chloroform/methanol (2:1) for 15 min and dried in vacuo. Quantitation of phosphate was performed by the method of Ames (1966).

Results

Identification of the SAC1p

Nucleotide sequence analysis of *SAC1* identified an open reading frame with the potential to encode a 623 residue polypeptide with a predicted molecular mass of some 71 kD (Cleves et al., 1989). We used this nucleotide sequence information to engineer the high level production of a TrpE-SAC1p fusion protein in *E. coli* which was then partially purified and used as immunogen for the generation of mouse mAbs (see Materials and Methods). To identify SAC1p, the appropriate yeast strains were radiolabeled with [^{35}S]-labeled amino acids for 30 min at 25°C, and SAC1p immunoreactive species were precipitated from the corresponding clarified extracts with a mixture of these two monoclonal antisera (see Materials and Methods). Vacuolar proteinase A (PrA) antigen, a control glycoprotein, was also monitored in these experiments so as to normalize the SAC1p data. The immunoprecipitates were resolved by SDS-PAGE and evaluated by autoradiography.

As the data in Fig. 1 (lane *B*) show, two labeled species were recovered from wild-type yeast lysates treated with both SAC1p and PrA antibodies: a 65-kD species and the 43-kD PrA. The 65-kD species was not recovered from wild-type lysates when preimmune serum was substituted for SAC1p antibodies in the precipitation assay (Fig. 1, lane *A*), nor was it recovered when SAC1p and PrA antibodies were reacted with lysate prepared from a Δ*sac1* strain (Fig. 1, lane *C*). Substantially increased amounts of the 65-kD species (relative to PrA) were recovered from extracts prepared from a yeast strain carrying *SAC1* on a multicopy plasmid; a strain expected to overproduce the SAC1p (Fig. 1, lane *D*). By densitometry, we estimate this level of overproduction to be approximately 20-fold relative to wild-type levels. Finally, pretreatment of wild-type yeast lysate with *E. coli* extract containing the TrpE-SAC1p fusion protein, against which the SAC1p antibodies were raised, specifically competed precipitation of the 65 kD species (Fig. 1, lane *F*). Challenge of the same wild-type lysate with an equivalent amount of *E. coli* extract that was devoid of SAC1p antigen exerted no such competitive effect (Fig. 1, lane *E*). The combined data demonstrate that the 65-kD species represents the SAC1p. Further confirmation of this conclusion is presented in Fig. 8 *A* where we show that several *sac1*^{cs} alleles encode what appear to be truncated forms of SAC1p (see below). In vivo radiolabeling experiments (coupled with quantitative immunoprecipitation, SDS-PAGE, autoradiography, quantitation by laser densitometry, and consideration of the rather modest differences in the sulfur-containing amino acid content of these two proteins) suggest that the SEC14p is some 15–20-fold more abundant than the SAC1p (See Fig. 3 *B*, lane 2). Since SEC14p represents a moderately abundant yeast cell protein (ca. 0.03% of total cell protein; Bankaitis et al., 1989), the data identify the SAC1p as a rather inabundant yeast protein.

To determine whether the SAC1p is a glycoprotein, cell-free lysates prepared from the SAC1p-overproducing strain

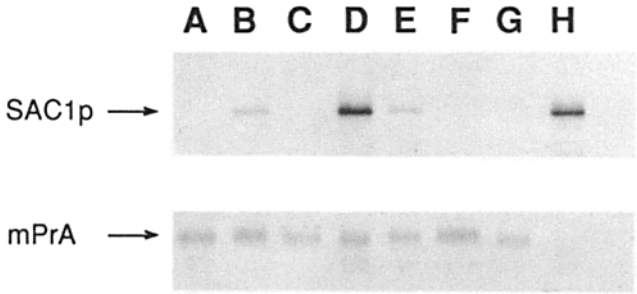

Figure 1. Identification of SAC1p. Strains CTY182 (*SAC1*), CTY244 (Δ*sac1*), and CTY150 (YEp *SAC1*) were grown in minimal medium and allowed to incorporate [^{35}S] Trans-label for 30 min at 30°C. Clarified extracts were prepared and analyzed by quantitative immunoprecipitation with anti-proteinase A (PrA) serum and, with the exception of lane *A* where preimmune SAC1p serum was used, monoclonal SAC1p antibodies. Immunoprecipitates were resolved by SDS-PAGE and autoradiography. Lane *A*, CTY182 and preimmune SAC1p serum; lane *B*, CTY182; lane *C*, the Δ*sac1* strain CTY244; lane *D*, the SAC1p overproducing strain CTY150; lane *E*, CTY182 with the addition of *E. coli* extract derived from cells not induced for synthesis of TrpE-SAC1p antigen; lane *F*, CTY182 with the addition of TrpE-SAC1p antigen against which the SAC1p antibodies were raised; lane *G*, the Con A–bound fraction prepared from clarified lysates derived from the SAC1p-overproducing strain CTY150; lane *H*, the Con A supernatant fraction prepared from CTY150 lysate. SAC1p and mature PrA (*mPrA*) are indicated at left.

were incubated with Con A–coated Sepharose beads, Con A-precipitable and supernatant fractions were generated, SAC1p and PrA were precipitated from each fraction, and the corresponding immunoprecipitates were evaluated by SDS-PAGE and autoradiography. As shown in Fig. 1 (lane *G*), PrA exhibited the expected behavior for a glycoprotein and was recovered only from the Con A–bound fraction. By contrast, SAC1p failed to bind the Con A beads and was recovered only from the supernatant fraction (Fig. 1, lane *H*). Taken together, these data demonstrate that SAC1p is an unglycosylated polypeptide, with an apparent molecular mass of some 65 kD, that is expressed at rather low levels in wild-type yeast cells.

The SAC1p Is An Integral Membrane Protein

Inspection of the inferred SAC1p primary sequence reveals a run of 23 uncharged amino acids, extending from residue 522 to residue 544, that constitutes a potential membrane-spanning domain (Cleves et al., 1989). To determine if SAC1p is membrane associated, we used a differential centrifugation regimen to resolve radiolabeled cell-free lysates into various membrane-enclosed and cytoplasmic fractions (see Materials and Methods). These fractions were then probed for SAC1p immunoreactive materials by quantitative immunoprecipitation with SAC1p mAb. PrA was also immunoprecipitated from these fractions. The conditions of radiolabeling were such that a significant percentage of the total radiolabeled PrA was recovered in the p1 and p2 forms of the enzyme. These forms of the PrA zymogen served as soluble lumenal markers for the ER and early Golgi, and late Golgi compartments, respectively (Klionsky et al., 1988).

As shown in Fig. 2 *A*, the p1 and p2 forms of PrA were nearly quantitatively recovered from the 12,000 *g* (P12) and 100,000 *g* (P100) pellet fractions, and no detectable amounts of p1 or p2 PrA were recovered from the 100,000 *g* supernatant (S100; i.e., cytoplasmic) fraction. These data indicate that the cell lysis procedure preserved the integrity of the yeast ER and Golgi. SAC1p exhibited a fractionation profile that was very similar to that observed for p1 and p2 PrA. That is, SAC1p quantitatively sedimented with membranes, and was roughly equally distributed between the P12 and P100 fractions (Fig. 2 *A*). These data, coupled with our findings that SAC1p floats in equilibrium flotation gradients (see below), demonstrate an association of SAC1p with yeast membranes and rule out the possibility that the SAC1p simply pellets as a large protein aggregate.

To investigate the membrane association properties of SAC1p, we determined whether alkaline pH treatment releases SAC1p from membranes (Fugiki et al., 1982). In these experiments we used strain CTY150, the SAC1p overproducing strain, to facilitate detection of the SAC1p. SEC14p served as a peripheral membrane protein/cytosolic protein control (Bankaitis et al., 1989). As expected, SEC14p was efficiently extracted by the alkaline treatment and was recovered only from the S100 fraction (Fig. 2 *B*). By contrast, SAC1p was recovered exclusively from the P100 fraction. Identical SAC1p extraction profiles were obtained when these experiments were performed with wild-type yeast strains (data not shown), thereby indicating that the membrane-association properties of SAC1p are not altered when the polypeptide is overproduced. In other experiments, we found that the majority (ca. 80%) of the SAC1p partitioned

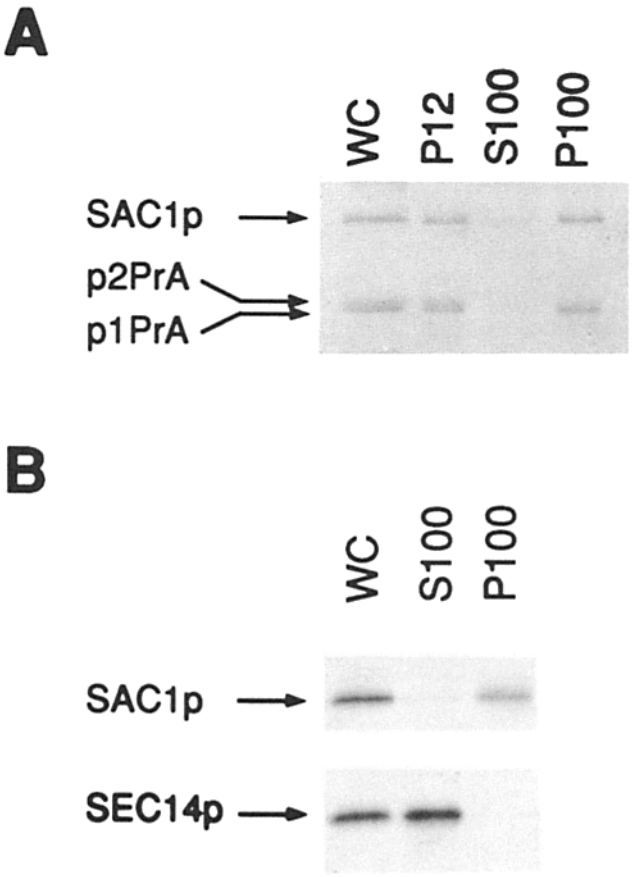

Figure 2. Membrane association properties of SAC1p. (*A*) Differential centrifugation. Strain CTY182 (*SAC1*) was radiolabeled and the resulting osmotic lysate was subjected to three rounds of centrifugation (see Materials and Methods). The whole cell (*WC*), 12,000 *g* pellet (*P12*), 100,000 *g* supernatant (*S100*), and 100,000 *g* pellet (*P100*) fractions were probed for the presence of precursor forms of PrA and SAC1p. The p1 and p2 PrA, indicated at left, serve as lumenal markers for ER and early Golgi, and late Golgi, compartments, respectively. Note that the WC fraction was derived from one-half of the material that was used to generate the other fractions (see Materials and Methods). Our recoveries of antigen after fractionation typically exceeded 85%. (*B*) Alkaline nonextractability of SAC1p. The SAC1p overproducing strain CTY150 was radiolabeled and an osmotic lysate was prepared. One-half of that cell-free lysate was saved as the whole cell (*WC*) fraction and the remainder was adjusted to 0.1 M Na_2CO_3 (pH 11.5). After a 1-h incubation on ice, the Na_2CO_3 fraction was centrifuged at 100,000 *g* and the resulting S100 and P100 fractions were probed for the presence of SAC1p and SEC14p, a peripheral membrane protein control.

into the detergent phase upon solubilization of osmotic lysates with Triton X-114 and subsequent resolution of aqueous and detergent phases (data not shown). These data indicate that SAC1p is an integral membrane protein.

Localization of the SAC1p by Immunofluorescence

To detect SAC1p by immunofluorescence methods, we used an antibody sandwich method that had previously been successfully applied to the localization of other inabundant yeast proteins (Pringle et al., 1989). Visualization of the SAC1p staining profile of wild-type yeast cells revealed a faint, but reproducible, punctate pattern (Fig. 3 *A*, lane 2). Further ex-

amples of this SAC1p staining profile are shown in Figs. 4 and 5. We generally observed between three and eight FITC-stained bodies per cell in any given focal plane, and >90% of the yeast cells exhibited this pattern. This punctate staining was not associated with either the nucleus or the mitochondria, as judged by the lack of colocalization of FITC-stained structures with DAPI-stained structures (Fig. 3 *A*, lane *2*). We address the identity of these punctate structures below. Moreover, we occasionally found cells that, in addition to the punctate staining, also exhibited what appeared to be a fainter nuclear envelope staining for SAC1p. An example of such SAC1p staining is presented in Fig. 4 (panel *2*). Those punctate and nuclear envelope SAC1p staining profiles are considered to reflect the authentic distribution of the SAC1p as *sac1*° yeast strains failed to exhibit any detectable FITC-staining under these experimental conditions (Fig. 3 *A*, lane *1*). Furthermore, preincubation of SAC1p antibodies with TrpE-SAC1p fusion protein, but not TrpE anti-

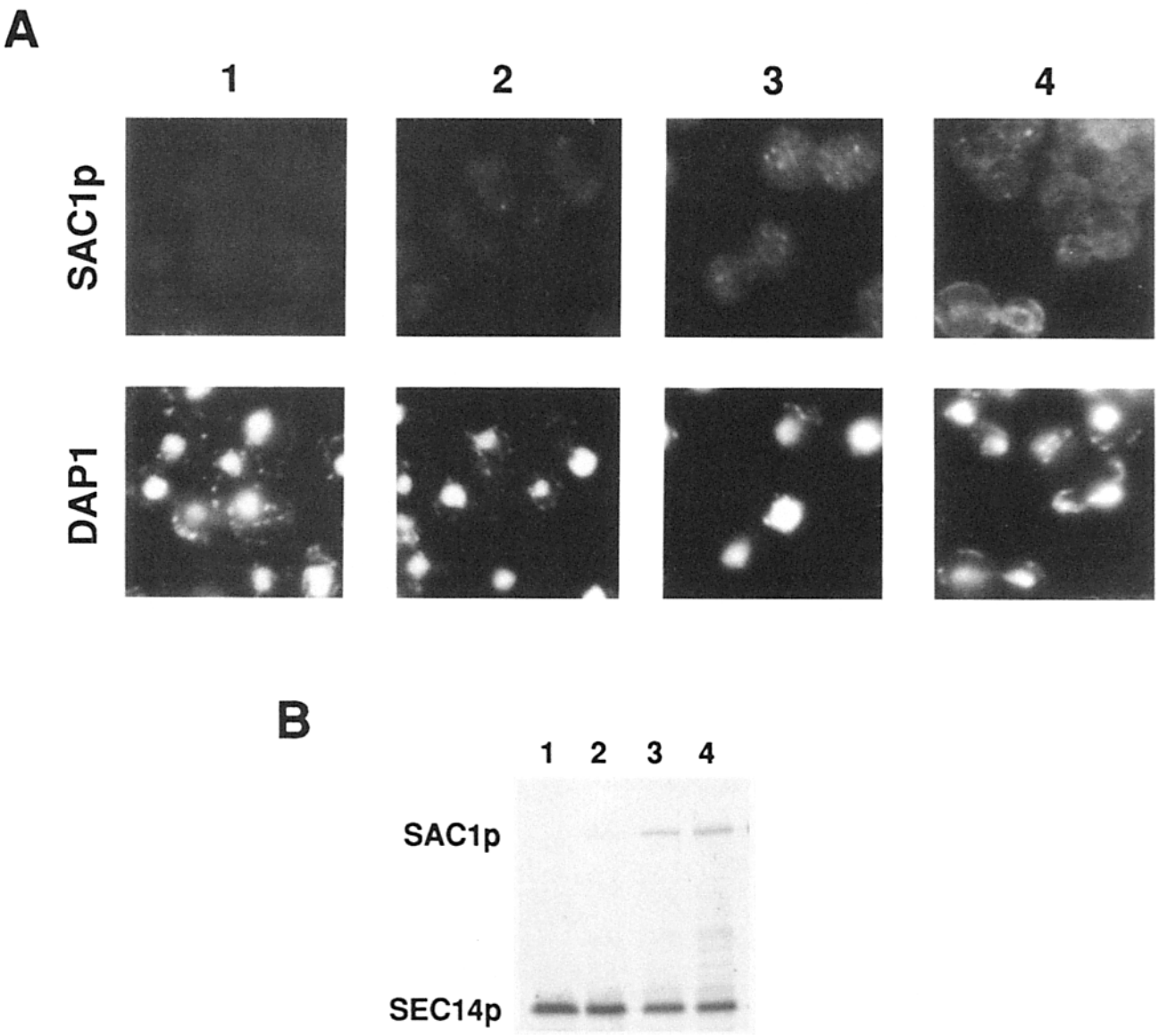

Figure 3. Localization of SAC1p. (*A*) Immunofluorescence localization of SAC1p. Fixed yeast cells were permeabilized and stained for SAC1p using an antibody sandwich consisting of primary anti-SAC1p mouse mAbs, secondary rabbit anti-mouse IgG serum, and tertiary goat anti-rabbit IgG conjugated to fluorescein isothiocyanate (FITC). Nuclei and mitochondria were stained with the DNA stain DAPI. Isogenic yeast strains engineered to produce varying relative amounts of SAC1p were employed in these experiments. Lane *1*, strain CTY463 (Δ*sac1*); lane *2*, strain CTY182 (*SAC1*); lane *3*, strain CTY444 (YEp *SAC1*); lane *4*, strain CTY443 (YCp *SAC1*). The YEp(*SAC1*) plasmid in strain CTY444 (i.e., pCTY114) harbors a 2.4-kb XbaI fragment that bears a promoterless, albeit otherwise intact, *SAC1* gene (Cleves et al., 1989). The YCp(*SAC1*) plasmid carried by strain CTY443 (i.e., pCTY101) harbors a 7.5-kb SstI-SphI genomic DNA fragment that includes the entire *SAC1* gene and the complete *SAC1* promoter. Both pCTY101 and pCTY114 carry *URA3* as a selectable marker. (*B*) Quantitation of relative SAC1p amounts. The corresponding yeast strains used in the immunofluorescence experiments described in the legend to Fig. 3 *A* were radiolabeled for 30 min at 30°C, clarified extracts were prepared from the corresponding TCA precipitates, and SAC1p and SEC14p immunoreactive materials were recovered by quantitative immunoprecipitation and resolved by SDS-PAGE and autoradiography. The SEC14p signal served to normalize the SAC1p data. The lane designations correspond exactly to those in Fig. 3 *A*.

gen alone, led to a complete loss of SAC1p signal in wild-type yeast cells that were subjected to this immunofluorescence regimen (data not shown).

The nuclear envelope component of SAC1p immunostaining became more pronounced when the amount of SAC1p produced by yeast cells exceeded wild-type levels. Yeast strains CTY444 and CTY443 were engineered to exhibit a modest overproduction of the SAC1p (see Materials and Methods). Quantitative immunoprecipitation analysis revealed that these strains overproduce SAC1p some three- and sixfold relative to wild-type, respectively (Fig. 3 *B*, lanes *3* and *4*). Strain CTY444 exhibited a predominantly punctate SAC1p-staining pattern that was very similar to that observed for wild-type cells, only more intense (Fig. 3 *A*, compare lanes *2* and *3*). By contrast, when CTY443 was analyzed by immunofluorescence, both punctate and nuclear envelope SAC1p-staining profiles were observed in essentially all of the cells (Fig. 3 *A*, lane *4*). Comparison of the FITC- and DAPI-staining patterns recorded for strain CTY443 demonstrate coincidence of the nuclear envelope with SAC1p staining. Furthermore, treatment of either wild-type or SAC1p-overproducing yeast strains with cycloheximide for 1 h before fixation did not alter the corresponding SAC1p localization profiles of these strains (not shown). Thus, no net chase of nuclear envelope SAC1p staining into punctate staining was observed, nor vice versa. We currently interpret these data to suggest two compartments of steady-state residence for the SAC1p in the yeast cell, and consider the nuclear envelope-associated SAC1p staining to likely reflect some localization of this polypeptide to the yeast ER system. This conclusion is based on the similarity of this pattern of SAC1p staining to the profile previously described for the lumenal ER marker KAR2p (Rose et al., 1989), and is further supported by subcellular fractionation experiments (see below). We also note that, under conditions of modest SAC1p overproduction, apparent SAC1p staining of the plasma membrane could occasionally be observed (see Fig. 3 *A*, panel *4*). On the basis of experimental evidence presented below,

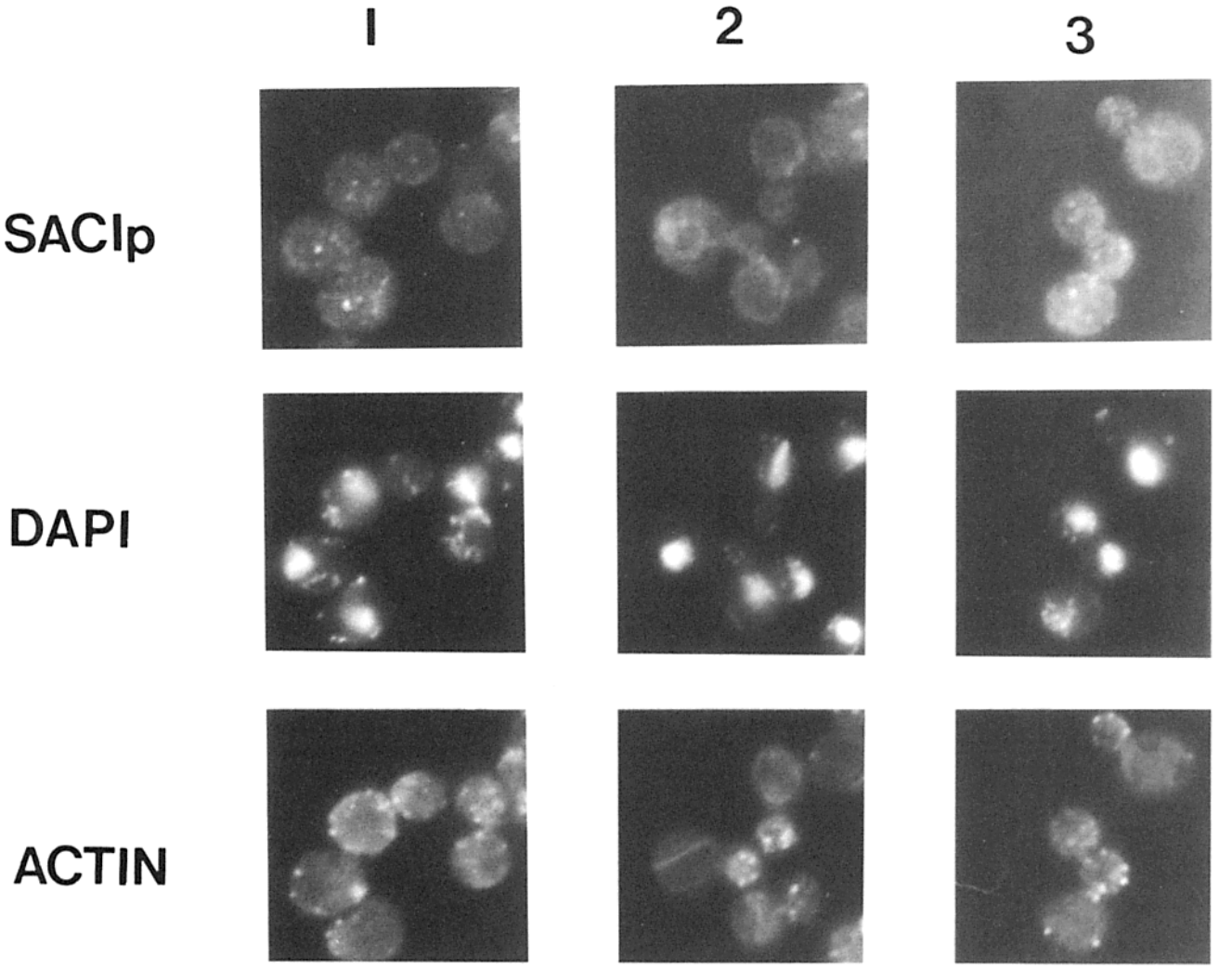

Figure 4. Double-label immunofluorescence staining of the filamentous actin cytoskeleton and SAC1p in yeast. Strain CTY443 was prepared for immunofluorescence as described in Materials and Methods. The F-actin cytoskeleton was stained with phalloidin conjugated to tetramethylrhodamine isothiocyanate (TRITC). The SAC1p was visualized using an antibody sandwich consisting of anti-SAC1p mAbs, rabbit anti-mouse IgG, and goat anti-rabbit IgG conjugated to fluorescein isothiocyanate (FITC). Nuclei and mitochondria were stained with DAPI.

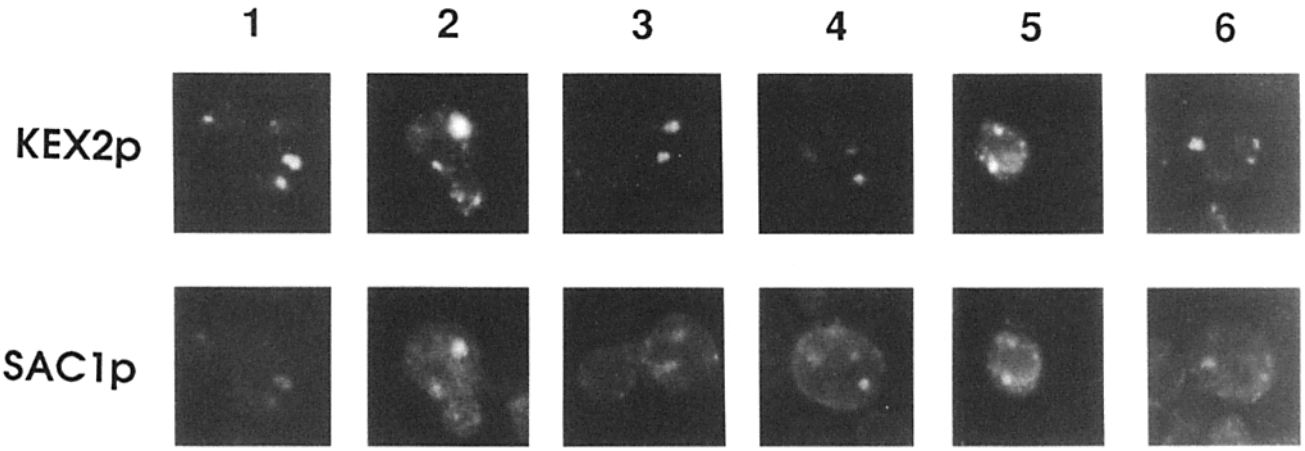

Figure 5. Colocalization of SAC1p with the yeast Golgi marker KEX2p. Yeast strain CTY234 was prepared for immunofluorescence as described in Materials and Methods. KEX2p was stained with primary rabbit polyclonal anti-KEX2p serum and secondary FITC-conjugated goat anti-rabbit IgG serum. SAC1p was stained using an antibody sandwich consisting of anti-SAC1p mouse monoclonal primary antibodies, sheep anti-mouse IgG secondary antibodies, and Texas red sulfonyl chloride (TRSC)-conjugated donkey anti-sheep IgG tertiary antibodies.

we believe this component of SAC1p staining to reflect the presence of SAC1p in the peripheral ER that lies immediately underneath the plasma membrane (Kaiser and Schekman, 1990).

SAC1p Does Not Detectably Associate with the Bulk of the Yeast F-Actin Cytoskeleton

To determine whether the punctate aspect of SAC1p immunofluorescence staining represents localization of SAC1p to plasma membrane-associated patches of filamentous- (F-) actin, termed cortical actin patches (Kilmartin and Adams, 1984), we performed a series of double-label immunofluorescence experiments.

Yeast cells were fixed, permeabilized, and stained for SAC1p by the antibody sandwich technique described above using an FITC-conjugated tertiary antibody. The cells were then co-stained with TRITC-conjugated phalloidin, a probe for F-actin. Visualization of the rhodamine staining profile of these wild-type yeast cells revealed the actin cables and cortical actin patches of the F-actin cytoskeleton in yeast (Fig. 4; Kilmartin and Adams, 1984). The cortical actin patches are represented by the punctate F-actin staining that is prominently displayed in panels *1–3* of Fig. 4. These cortical patches were not coincident with either the SAC1p punctate staining profile, as determined by FITC fluorescence, or nuclear and mitochondrial staining, as determined by DAPI fluorescence. Furthermore, the actin cables, most prominently featured in panel *2*, were not arranged in a manner that suggested some extensive association with SAC1p punctate or perinuclear staining. These data indicate that: (*a*) SAC1p was not localized to cortical actin patches, and (*b*) that SAC1p did not exhibit some global association with the F-actin cytokeleton; at least not within the limits of detection of this technique. However, we were able to co-recover, in a SAC1p-dependent manner, both SAC1p and actin from cell-free lysates by native immunoprecipitation using either affinity-purified actin-specific antibodies or monoclonal SAC1p antibodies as affinity probes (data not shown). The difficulties of absolutely excluding some artifactual co-recovery of SAC1p with the abundant actin polypeptide in such experiments, coupled with the failure of initial attempts to recover SAC1p/actin complexes in cross-linking experiments, preclude a firm interpretation of those co-precipitation data. Nevertheless, such data leave open the possibility that SAC1p associates with G-actin or actin oligomers in vivo.

SAC1p Localizes to Yeast Golgi

To investigate the possibility that the punctate bodies stained with SAC1p antibodies represent yeast Golgi bodies, we assessed the co-localization of SAC1p with KEX2p, an integral membrane protein of the yeast Golgi (Franzusoff et al., 1991; Redding et al., 1991). Strain CTY234, a KEX2p overproducing strain, was used for those studies. Fuller and colleagues have shown that yeast bearing the *KEX2* gene on a multicopy plasmid exhibit normal localization for KEX2p, and that the amplified KEX2p staining can be readily detected without having to resort to antibody sandwich methods (Franzusoff et al., 1991; Redding et al., 1991). To visualize KEX2p, fixed, and permeabilized cells of strain CTY234 were incubated with affinity-purified rabbit polyclonal anti-KEX2p serum and FITC-conjugated goat anti-rabbit IgG. SAC1p was detected using an antibody sandwich consisting of primary anti-SAC1p mouse mAbs, sheep anti-mouse IgG, and developed with Texas Red sulfonyl chloride (TRSC)-conjugated donkey anti-sheep IgG. Appropriate controls were performed to insure the specificity of the antisera and to verify the spectral separation of the fluorochromes under the photographic conditions employed (not shown). Fig. 5 shows representative cells from the ~100 cells that were examined in these studies. The upper panels show the punctate staining that is characteristic of KEX2p localization (Cleves et al., 1991; Franzusoff et al., 1991; Redding et al., 1991), and the lower panels show the corresponding SAC1p localization in the same cells. Inspection of these cells revealed a significant, but not absolute, coincidence of SAC1p and KEX2p staining bodies (Fig. 5). We estimate that >50% of the punctate SAC1p-staining bodies scored positive for KEX2p, and vice versa.

The biochemical cofractionation of SAC1p with two Golgi

A

Fraction	SAC1p	KEX2p	SEC14p	CC RED
S1	215266	99742	1287	5.703
(%S1)	100%	100%	100%	100%
S12	107479	72342	790	2.142
(%S1)	50%	73%	61%	38%
P12	101918	20881	468	2.589
(%S1)	47%	21%	36%	45%
S100	276	1791	578	0.015
(% S1)	>1%	2%	45%	>1%
P100	103199	67695	272	1.896
(%S1)	48%	68%	21%	33%
GRAD #1	96920	59760	236	1.380
(%S1)	45%	60%	18%	24%
GRAD #2	55535	56940	152	0.036
(%S1)	26%	57%	12%	>1%

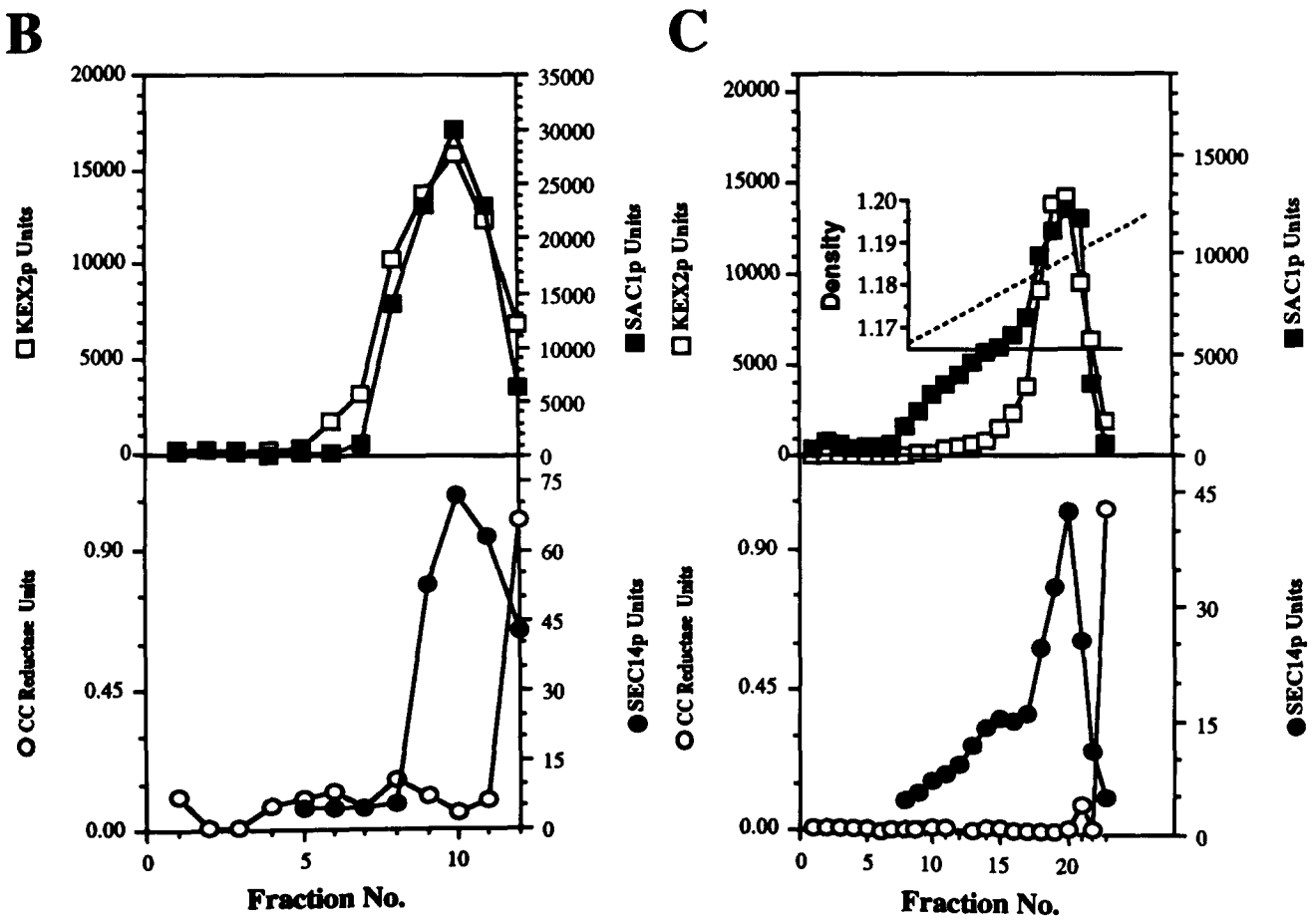

Figure 6. Quantitation of SAC1p in highly enriched Golgi fractions. (*A*) Distribution of marker proteins in supernatant and pellet fractions. Wild-type (CTY182) cells were grown at 25°C in YPD medium, converted to spheroplasts, and osmotic lysates prepared and fractionated essentially as previously described (Cleves et al., 1991). The P100 fraction was further resolved by equilibrium flotation centrifugation in a 40–65% sorbitol gradient and 1.0-ml fractions were collected from the top and assayed for the appropriate markers. The KEX2p peak fraction pool from this first gradient was designated the GRAD#1 fraction and was then further resolved by equilibrium sedimentation centrifugation in a second 50–60% sorbitol gradient, 0.5-ml fractions were collected from the top, and analyzed for the indicated markers. The KEX2p peak fraction pool from this second gradient was designated as the GRAD#2 fraction. The relative quantities of KEX2p, SEC14p, and SAC1p in each fraction were determined by quantitative ELISA (see Cleves et al., 1991*b*) using 1.66 μg/ml, 5.7 μg/ml, and 2.24 μg/ml of antibody, respectively. Enzyme activities of the ER marker NADPH cytochrome c reductase (*CC RED*) are expressed as umoles of cytochrome c reduced per min per fraction. (*B* and *C*) Graphic representation of marker protein distribution across the first 40–65% and second 50–60% sorbitol gradients, respectively.

markers, KEX2p and SEC14p, was assessed by a modification of a method we have previously described for obtaining highly enriched yeast Golgi fractions that are substantially free of contamination by the plasma membrane or ER, vacuolar, and mitochondrial membranes (Cleves et al., 1991*b*). We also monitored the distribution of an ER marker, NADPH cytochrome c reductase, throughout the fractionation. The data presented in Fig. 6 *A* show that most of the KEX2p (68% of total) was recovered in the P100 fraction. The SAC1p, SEC14p, and cytochrome c reductase distributed more equally between the P12 and P100 membrane fractions. Further resolution of the P100 fraction by equilibrium flotation in a self-forming 40-65% sorbitol gradient demonstrated coincidence of the peak KEX2p, SEC14p and SAC1p fraction pools (Fig. 6 *B*), containing 60, 18, and 45% of total material, respectively. Moreover, satisfactory recoveries of antigen were obtained as 88, 86, and 94% of input material was recovered from the peak fraction pools for KEX2p, SEC14p, and SAC1p, respectively. Most of the cytochrome c reductase was recovered from denser fractions and some was pelleted to the bottom of the tube as well. Although the peak cytochrome c reductase fractions could be distinguished from the peak KEX2p, SEC14p and SAC1p fractions (Fig. 6 *B*), the fractions were pooled in such a manner that some 24% of the total cytochrome c reductase was still present in the KEX2p/SEC14p/SAC1p peak fraction. The final step involved resolution of the pooled membranes by equilibrium sedimentation in a self-forming 50–60% sorbitol gradient. Again, the KEX2p, SEC14p and SAC1p peak profiles in the sedimentation gradient were largely coincident (Fig. 6 *C*) although the SEC14p and SAC1p peaks each exhibited a trail into lighter fractions whereas the KEX2p peak did not. Indeed, the SEC14p and SAC1p peak profiles were nearly superimposable. Some 57% of the total KEX2p (95% of input) was recovered in the peak KEX2p fractions collected from this gradient, and 26% of the total SAC1p (58% of input) was recovered in those KEX2p peak fractions. Approximately 94% of the input SAC1p was recovered in the SAC1p-containing fractions of this gradient. Cytochrome c reductase sedimented quantitatively to the bottom of the gradient, and <1% of total reductase was recovered in the KEX2p peak fractions. Thus, a significant percentage of the total SAC1p coenriched with the yeast Golgi integral membrane protein marker KEX2p and the peripheral Golgi protein SEC14p.

SAC1p Also Resides in the Yeast ER

As approximately 50% of the total cellular SAC1p was recovered in the P12 fraction, along with the majority of the ER and plasma membrane markers (i.e., NADPH cytochrome c reductase and plasma membrane ATPase, respectively; Fig. 6 *B* and Cleves et al., 1991*b*), we further fractionated the P12 to assess the distribution of the SAC1p with respect to ER and plasma membrane markers. The P12 was generated as described above, and determined to contain 54, 63, 43, and 8% of the total cytochrome c reductase, plasma membrane ATPase, SAC1p, and KEX2p, respectively (data not shown). The P12 was then further resolved by equilibrium flotation in a self-forming 30–55% sucrose gradient by the method of Bowser and Novick (1991). Representative data are shown in Fig. 7. In this system, we were able to partially resolve ER from plasma membrane fractions. The cytochrome c reductase was primarily localized to two distinct peaks. Approximately 20% of the total cytochrome c reductase was recovered in the less dense peak pool (fractions 11–15), whereas 19% of the total was recovered in the denser peak pool (fractions 16–19). This 39% recovery of total cytochrome c reductase in these two peaks represented a 91% recovery of enzyme loaded into the gradient. The plasma membrane ATPase fractionated in a single peak (fractions 18–22) that contained 31% of the total plasma membrane ATPase (49% of input) and was denser than the ER peaks. The minor cellular fraction of KEX2p present in the P12 came off the gradient in a single peak (fractions 9–12) that was less dense than any of the ER and plasma membrane peaks (Fig. 7). These profiles are in good agreement with those reported by Bowser and Novick (1991). SAC1p was recovered primarily in a single peak that encompassed fractions 15–20 and contained 20% of total SAC1p (48% of input). This peak coincided almost exactly with the denser of the two cytochrome c reductase peaks. Indeed, some 17% of the total cellular SAC1p (40% of input) was recovered in

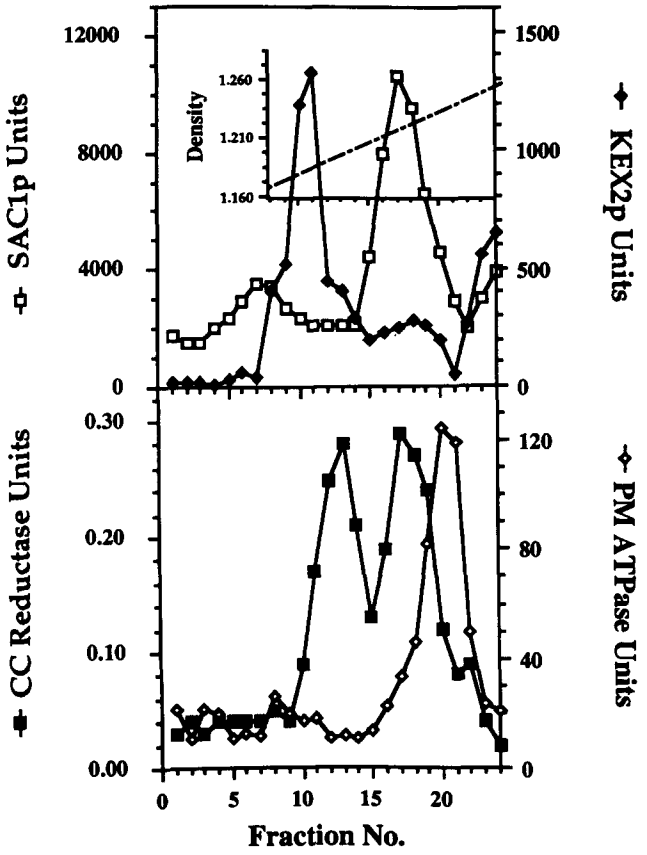

Figure 7. SAC1p cofractionates with ER membranes. P12 fractions were generated as described in the legend to Fig. 6 *A*, and the fraction of total intracellular NADPH cytochrome c reductase, vanadate sensitive plasma membrane ATPase, KEX2p, and SAC1p in the P12 was determined as described (Cleves et al., 1991*b*). The P12 was subsequently resolved by equilibrium flotation in a self-forming 30–55% sucrose gradient by the method of Bowser and Novick (1991), 0.5-ml fractions were collected from the top of the gradient to the bottom, and the various markers were quantitated in each fraction. The relative activities, or quantities, of each marker are expressed on a per 1-ml fraction.

the dense reductase pool (fractions 16–19). A significant amount of SAC1p (11% of total; 26% of input) was recovered in the plasma membrane fractions as well (Fig. 7). We note, however, that ~15% of total cytochrome c reductase (34% of input) was also recovered from those peak plasma membrane fractions (18–22). As a result, the contamination of plasma membrane fractions by ER can fully account for SAC1p detected in those fractions. Since we have failed to gain access to SAC1p by protease shaving of intact spheroplasts, or by extrinsic labeling of surface exposed proteins by radioiodination methods (not shown), we consider the collective data to be most consistent with a localization of SAC1p to a subfraction of ER membranes, in addition to Golgi membranes.

Suppression of SEC14p and Actin Defects Occurs Through Loss of SAC1p Function

The *sac1* null (*sac1°*) phenotype is cold sensitivity for growth (Novick et al., 1989; Cleves et al., 1989). Since all of the available *sac1* alleles render the corresponding mutant strains *cs* for growth, regardless of whether these alleles were initially identified as suppressors of *act1-1ts* or of *sec14-1ts*, it seems likely that suppression in both cases involves loss of SAC1p function. However, the finding that *sac1°* mutations result in a phenotypically less efficient suppression of *act1-1ts* or *sec14-1ts* lesions has prompted the suggestion that suppressor *sac1cs* alleles attenuate, but may not eliminate, SAC1p function (Novick et al., 1989; Cleves et al., 1989). As a resolution of this issue is crucial to the understanding of how SAC1p relates to both actin and Golgi function in yeast, we wished to examine this point further by analyzing the SAC1p profile from 21 representative *sac1cs* strains. Fourteen of the corresponding alleles were isolated as suppressors of *sec14-1ts* whereas the remaining seven were identified as suppressors of *act1-1ts*. The appropriate strains were radiolabeled for 1 h at 30°C with ^{35}S-labeled amino acids, SAC1p and SEC14p immunoreactive materials were recovered, and the products were analyzed by SDS-PAGE, and autoradiography. The SEC14p signal served to normalize the SAC1p data.

The *sac1cs* mutations fall into three general classes with respect to the form of SAC1p that was detected in lysates prepared from the corresponding mutants. Representative data for each of these classes are shown in Fig. 8 *A*, while a comprehensive tabulation of the data is presented in Fig. 8 *B*. Class I is represented by six *sac1cs* alleles and the corresponding mutants exhibited a form of SAC1p that, by SDS-PAGE, was indistinguishable from wild-type SAC1p. Moreover, the amount of SAC1p antigen recovered from the class I mutants was not significantly reduced relative to that recovered from the wild-type strain. Class II mutants, however, produced a truncated form of SAC1p, and four *sac1cs* alleles fall into this category. The SAC1p species encoded by the three class II alleles represented in Fig. 8 *A* (i.e., *sac1-6cs*, *sac1-11cs*, *sac1-14 cs*) exhibited molecular masses of ~53 kD, 52 kD, and 55 kD, respectively. Finally, the remaining 11 *sac1cs* alleles define the class III category. The corresponding mutants failed to produce detectable SAC1p antigen under the radiolabeling conditions described. Since these experiments involved a relatively long period of radiolabeling (1 h), we have also attempted to visualize SAC1p antigen in class III mutants under conditions of pulse-radiolabeling.

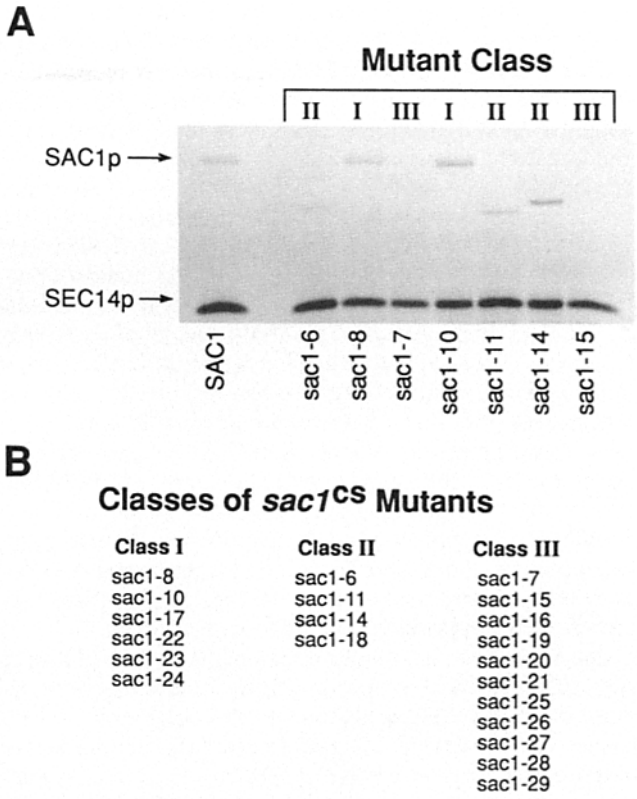

Figure 8. SAC1p profiles of *sac1cs* yeast. (*A*) The appropriate yeast strains were radiolabeled for 1 h at 30°C and converted to clarified extracts after termination of labeling by addition of TCA to a final concentration of 5%. These extracts were then probed for SAC1p and SEC14p antigen by quantitative immunoprecipitation, SDS-PAGE, and autoradiography. The SEC14p signal served to normalize the SAC1p data. Relevant genotypes are indicated at bottom. Mutant classes are as follows: class I, Sac1p^{cs} migrated as a full-length species; class II, Sac1p^{cs} behaved as a truncated polypeptide on SDS-PAGE; class III, no detectable SAC1p antigen was recovered. (*B*) Tabulation of *sac1cs* mutant classes. The 21 *sac1cs* alleles analyzed for SAC1p profile are categorized by the classification described in the legend to Fig. 8 *A*.

We have used pulse radiolabels of as short as 5 min and still have failed to detect SAC1p antigen in those mutant lysates. This inability to detect SAC1p antigen in class III *sac1cs* strains is considered significant as the wild-type SAC1p exhibits a half-life of ~1 h at 30°C (not shown). The simplest interpretation of these collective data is that the class III *sac1cs* alleles are essentially equivalent to *sac1°* alleles, and these data are most consistent with a model in which the mechanism of *act1-1ts* and *sec14-1ts* suppression involves loss of SAC1p function. This model predicts that *sac1* disruption mutations should result in a bypass of the normally essential SEC14p requirement and, consequently, a suppression of *sec14* disruption alleles. This prediction was fulfilled by our ability to directly transplace the haploid-lethal *sec14-129::HIS3* disruption (described in Bankaitis et al., 1989) into *sac1°* haploid strains by transformation.

Suppression of SEC14p Defects is not a General Property of Mutations in SAC Genes

Previous work has identified other *SAC* genes, clearly distinct from *SAC1*, whose products represent candidate actin

binding proteins (Novick et al., 1989; Dunn and Shortle, 1990; Adams et al. 1989). As in the case of *SAC1*, the *SAC2* and *SAC3* genes were identified on the basis of the isolation of *cs* mutations that exhibit a recessive and allele-specific suppression of *act1*^{ts} mutations (Novick et al., 1989). *SAC7* was similarly identified in an actin suppressor screen and, while suppressor *sac7* alleles exhibit both co-dominant and recessive phenotypic traits, both the allele-specificity of the suppression of actin mutations and the synthetic lethality associated with specific combinations of *sac7* and *act1*^{ts} alleles closely resembles the genetic interactions observed between *sac1* and *act1*^{ts} alleles (Dunn and Shortle, 1990). *SAC6* was identified in a screen for dominant suppressors of *act1*^{ts} (Adams et al. 1989). Penetrating insights into the mechanism of function have been obtained for only one of these gene products. Adams et al. (1989) have provided strong evidence to indicate that the SAC6p is the yeast version of the actin bundling protein fimbrin. To determine if phenotypic suppression of *sec14* mutations is a general property of *sac* mutations, we combined the appropriate *sac* alleles with defined *sec14* alleles in haploid yeast and then scored phenotypic suppression of *sec14* defects.

The data show *sac1* alleles to be unique in their ability to suppress *sec14* defects. Introduction of the dominant suppressor of actin allele *sac6-2* had no effect on the cellular requirement for SEC14p function as evidenced by the failure of this dominant *sac6-2* allele to effect any detectable phenotypic suppression of *sec14-1*^{ts} or *sec14Δ1::HIS3*. Suppression of the normally lethal *sec14Δ1::HIS3* lesion was assessed by a plasmid shuffle/colony sectoring assay that tested whether a yeast centromeric plasmid bearing the *sac6-2* allele (i.e., pAAB162; see Adams et al., 1989) was able to relieve the dependence of a *sec14Δ1::HIS3* strain (CTY558; Table I) on the presence of a *SEC14* plasmid for viability (not shown). The recessive suppressor of actin alleles *sac2-1*^{cs} and *sac3-1*^{cs} also failed to phenotypically suppress *sec14-1*^{ts}, as judged by the uniform 2:2 segregation of Ts$^+$/Ts$^-$ phenotypes in the meiotic progeny obtained from each of the 10 and 12 asci analyzed from genetic crosses where *sec14-1*^{ts} and *sac2-1*^{cs}, and *sec14-1*^{ts} and *sac3-1*^{cs} were segregating, respectively. If these *sac*^{cs} alleles were to suppress *sec14-1*^{ts}, we would have expected the majority (ca. 75%) of asci to have yielded greater than two Ts$^+$ meiotic progeny apiece. Moreover, we readily recovered *sec14-1*^{ts}, *sac*^{cs} double mutant meiotic progeny from these crosses, as identified by their dual *ts,cs* phenotypes. Finally, a *sac7Δ1::URA3* null allele (see Materials and Methods), an allele that is directly analagous to a *sac7::LEU2* disruption allele shown by Dunn and Shortle (1990) to suppress actin defects, also was unable to effect a phenotypic suppression of either *sec14-1*^{ts} or *sec14Δ1::HIS3*. Again, suppression of the latter was assessed by testing whether a genomic *sac7Δ1::URA3* allele could relieve the dependence of a *sec14Δ1::HIS3* strain (CTY558; see Table I) on the presence of a *SEC14* plasmid for viability. Suppression of *sec14-1*^{ts} was assessed by transplacement of *sac7Δ1::URA3* into a haploid *sec14-1*^{ts} strain (CTY1-1A; Table I) and scoring the desired recombinants for phenotypic suppression of *sec14-1*^{ts} (see Materials and Methods).

Thus, *sac1* alleles are unique with respect to their ability to suppress both specific actin defects and wholesale defects in SEC14p function. The distinction between *sac1* and *sac7* mutations in this regard is especially noteworthy as *sac1* and *sac7* mutations exhibit a very similar allele specificity not only with respect to which actin mutations these suppress (i.e., *act1-1*^{ts}), but also with respect to which actin mutations (i.e., *act1-2*^{ts}) result in synthetic lethality when combined with these *sac* mutations in a haploid yeast cell (Novick et al., 1989; Dunn and Shortle, 1990).

sac1 Mutants are Inositol Auxotrophs

During the course of these studies, we noted that *sac1* mutants fail to grow in inositol-free media. As wild-type yeast strains have de novo inositol biosynthetic capability, this inositol auxotrophy represents a new *sac1*-associated phenotype and is illustrated in Fig. 9 *A*. The growth characteristics of a number of *sac1* strains on inositol-free and inositol supplemented media were compared to those of a *SAC1* strain and a known inositol auxotrophic strain (*inol-13*). The *inol-13* strain is deficient in inositol-1-phosphate synthase activity and fails to convert glucose-6-phosphate to inositol-1-phosphate, a direct intermediate in inositol biosynthesis in yeast (for a review see Carman and Henry, 1990). The data indicate that: (*a*) *sac1* strains failed to grow (i.e., form isolated colonies) on inositol-free medium; (*b*) the severity of this growth defect closely resembled that of the *inol-13* mutant; and (*c*) this growth defect was inositol remedial. The growth capabilities of the other *sac* mutants were also tested on media either containing or lacking inositol. The data are presented in Fig. 9 *B*. Clearly, all of the other *sac* mutants exhibited rather normal growth properties irrespective of the inositol content of the media. These phenotypic data indicate that *sac1* mutants are unique among the *sac* mutants not only in their suppression of *sec14* defects, but also in their inositol auxotrophy.

Measurement of Intracellular Inositol Pools in sac1 Mutants

Several indirect lines of evidence suggested that the inositol auxotrophy associated with *sac1* mutations was not likely to be the simple result of an inositol biosynthetic defect. Genetic mapping and nucleotide sequence data indicate that the structural genes for: (*a*) yeast inositol-1-phosphate synthase (*INO1*); (*b*) the transcriptional activators of *INO1* (i.e., *INO2* and *INO4*); and (*c*) *SAC1*, are clearly distinct (Donahue and Henry, 1981; Klig and Henry, 1984; Novick et al., 1989; Cleves et al., 1989; Hoshizaki et al., 1990; Nikoloff et al., 1992). Second, the *inol-13* allele fails to suppress *sec14-1*^{ts} and does not manifest itself in a *cs* growth phenotype (not shown). Finally, the *cs* growth defects and suppressor phenotypes associated with *sac1* mutations are manifested in media containing sufficient inositol to overcome any inositol biosynthetic defects.

To more directly assess whether *sac1* mutants suffer an intracellular inositol deficit when shifted to inositol-free media, we measured intracellular inositol pools in wild-type, *inol*, and *sac1* mutant strains as a function of inositol deprivation. As shown by the data in Fig. 10 *A*, the intracellular inositol pools of the wild-type, *inol-13*, and *sac1-26* mutant strains immediately after shift to inositol-free medium were of similar magnitude, ranging from ~2.5 nmoles inositol/μg protein in the case of the wild-type and *inol-13* strains down to 2.0 nmoles inositol/μg protein for the *sac1-26* mutant. Although these values were quite similar, we note that the inosi-

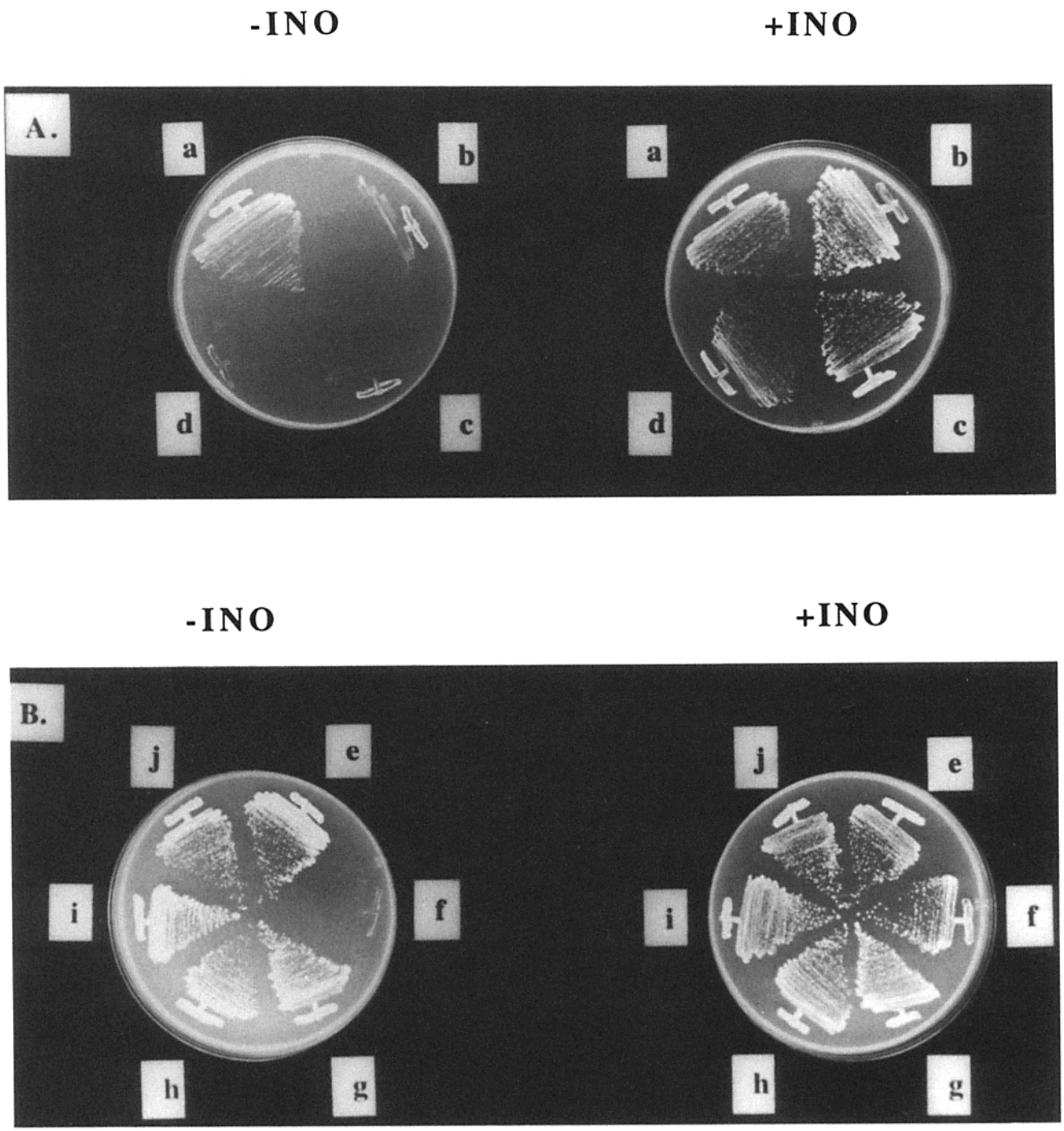

Figure 9. Inositol auxotrophy of *sacl*^{cs} mutant strains. The appropriate yeast strains were streaked for isolation on defined minimal medium either supplemented with inositol (+*INO*), or left unsupplemented (−*INO*), and incubated at 26°C for 96 h. The strains are as follows: (*a* and *e*) CTY182 (wild-type); (*b* and *f*) CTY417 (*inol-13*); (*c*) CTY100 (*sacl-26*); (*d*) CTY403 (*sacl-10*); (*g*) CTY567 (*sac2-1*); (*h*) CTY568 (*sac3-1*); (*i*) AAY1022 (*sac6-15*); and (*j*) CTY578 (*sac7Δ1::URA3*).

tol pools of the *sacl-26* mutant were slightly, but reproducibly, lower than those of the wild-type and *inol-13* strains. At this time we do not consider this to be a significant difference. Deprivation of wild-type cells for exogenous inositol for a 3-h period had no significant effect on intracellular inositol pools. In marked contrast, similar challenge of the *inol-13* mutant resulted in almost a 6-fold reduction in its inositol pools relative to those measured for this strain immediately after shift into inositol-free medium (Fig. 10 *A*). We presume that this loss of inositol pool homeostasis was a manifestation of the *inol-13*–associated inositol biosynthetic defect. As in the case of the wild-type strain, a 3 h inositol deprivation did not elicit any appreciable reduction in the inositol pools of the *sacl-26* mutant strain (Fig. 10 *A*). From these data we infer that *sacl* mutants were not defective in inositol biosynthesis.

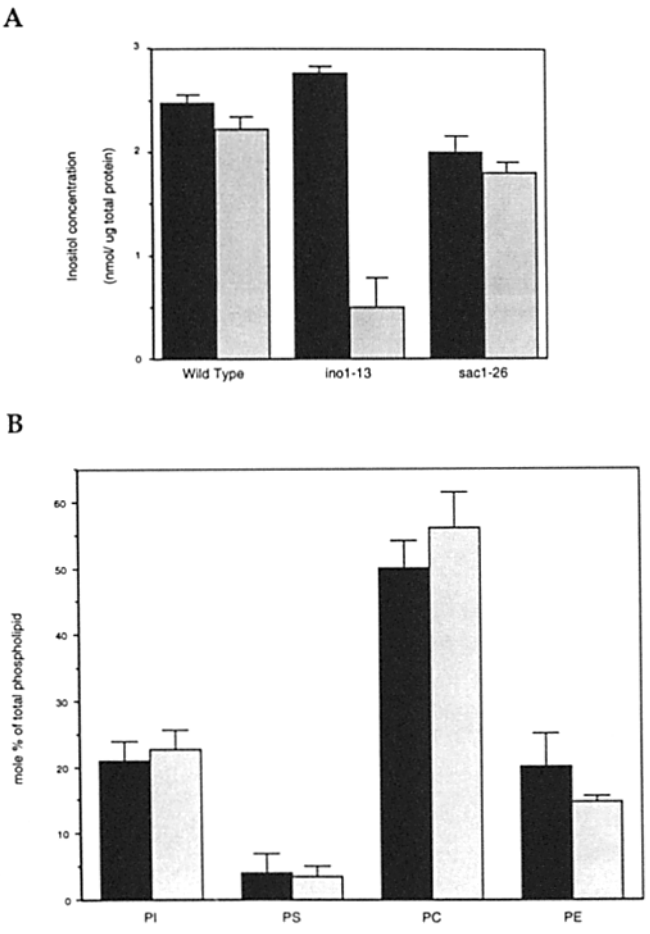

Figure 10. sacl yeast mutants are neither defective in inositol synthesis nor in inositol utilization. (*A*) Yeast strains CTY182 (*wild-type*), CTY417 (*inol-13*), and CTY100 (*sacl-26*) were grown in inositol supplemented minimal defined medium and subsequently shifted to inositol-free medium. Samples were harvested immediately after shift (0 min) and at 180 min postshift, and the inositol pools of the cells collected at each time point were determined for each strain as indicated (see Materials and Methods). Values for the 0 min sample are represented by the solid black bars whereas the 180-min samples are represented by the stippled bars. (*B*) Bulk membrane glycerophospholipid composition of wild-type and Δ*sacl* strains at steady state. Yeast strains CTY182 (*wild-type*) and CTY244 (Δ*sacl-296::HIS3*) were cultured in YPD. Total glycerophospholipid was subsequently extracted, resolved into individual species by two-dimensional chromatography, and the phosphate content of each species quantitated by chemical assay. The data for each individual phospholipid species are presented as mole % of the indicated species measured relative to total glycerophospholipid plus phosphate remaining at the origin. Values for the wild-type strain are represented by the solid black bars whereas the Δ*sacl* values are represented by the stippled bars. Phospholipid species are indicated as phosphatidylinositol (*PI*), phosphatidylserine (*PS*), phosphatidylcholine (*PC*), and phosphatidylethanolamine (*PE*).

Bulk Membranes Prepared From sacl Mutants Exhibit a Normal Phosphatidylinositol Content

To determine whether *sacl* mutants are somehow defective in the incorporation of inositol into PI, we compared the glycerophospholipid composition of bulk membranes prepared from wild-type and Δ*sacl* yeast. In these experiments, cells were cultured in YPD, an inositol-containing medium, total glycerophospholipids were extracted from the cells, displayed by two-dimensional paper chromatography, and individual glycerophospholipid species recovered and quantitated by inorganic phosphate assay (see Materials and Methods). As demonstrated by the data in Fig. 10 *B*, the steady-state bulk membrane glycerophospholipid compositions of the wild-type and Δ*sacl* mutant strains were very similar. Indeed, both strains exhibited essentially the same PI content as a function of total glycerophospholipid (ca. 22 mole%). Similar results were obtained when these same strains were radiolabeled to steady-state with [^{32}P]orthophosphate in phosphate-depleted YPD. Additional [^{32}P]orthophosphate pulse-radiolabeling experiments (30-min pulse) in phosphate-depleted YPD medium also failed to reveal obvious differences in bulk membrane PI content between wild-type and Δ*sacl* strains (not shown). These data suggest that *sacl* mutants were not grossly impaired in their ability to incorporate inositol into PI, and that *sacl* mutants did not experience wholesale defects in PL metabolism.

Discussion

Our data indicate a physical association of SAC1p with compartments of the secretory pathway. First, immunoprecipitation experiments identified SAC1p as an inabundant and unglycosylated protein with an apparent molecular mass of 65 kD (Fig. 1). Second, subcellular fractionation experiments demonstrated that SAC1p quantitatively sedimented with membranes (Fig. 2 *A*). Moreover, we found that SAC1p was not extracted from membranes by alkaline Na_2CO_3 treatment (Fig. 2 *B*) and, in other solubilization experiments, we observed that SAC1p efficiently partitioned into a Triton X-114 detergent phase. These data indicate that SAC1p is an integral membrane protein. Third, immunofluorescence analyzes revealed a predominantly punctate pattern for SAC1p staining in wild-type cells (Fig. 3 *A*, lane 2). Double-label fluorescence experiments indicated a substantial colocalization of the punctate SAC1p staining with structures stained with probes specific for KEX2p, a resident polypeptide of yeast Golgi membranes (Fig. 5), and biochemical fractionation data confirmed a significant presence of SAC1p in highly enriched Golgi fractions (Fig. 6; see above). Since it is the Golgi complex that is dysfunctional in *sec14* strains, and *sacl* mutations effect a bypass of the normally essential SEC14p requirement for yeast Golgi secretory function, these data suggest that SAC1p exerts a local effect on the secretory competence of yeast Golgi membranes. We note, however, that SAC1p-specific staining of what appears to be the yeast ER was also observed and that the prominence of this staining increased in direct proportion to the intracellular levels of SAC1p (Fig. 3 *A*). Subcellular fractionation experiments further confirmed the presence of SAC1p in a subfraction of ER membranes prepared from wild-type cells (Fig. 7). Thus, SAC1p exhibits a steady-state residence in the yeast Golgi complex and in the yeast ER. The latter component of SAC1p localization may provide some physical basis for the negative genetic interactions that have been observed between *sacl^{cs}* alleles and several *sec* mutations that block protein transport through early stages of the secretory pathway (Cleves et al., 1989). With regard to whether SAC1p associates with actin, we found that SAC1p staining was not ob-

viously coincident with that of cortical actin patches or actin cables (Fig. 4). Thus, the present data do not support models invoking some global association of SAC1p with the F-actin cytoskeleton. However, our ability to coprecipitate SAC1p and actin in native immunoprecipitation experiments still leaves open the possibility that SAC1p may associate with G-actin or actin oligomers in vivo (see above).

How can the various data be incorporated into a model for SAC1p function in vivo? Clearly, it is the loss of SAC1p function that results in the bypass of the normally essential SEC14p requirement and in the suppression of *act1-1*^{ts} (Fig. 8). These data indicate that SAC1p function is, in principle, antagonistic to both Golgi secretory function and some aspect of actin function (perhaps actin assembly) in yeast. Finally, the ability of *sac1* alleles to cosuppress both actin and *sec14* defects is a feature that is unique to *sac1* as this character was not exhibited by the several other suppressor of actin *sac* alleles we have tested. For this reason, we believe that the mechanism of suppression, by SAC1p dysfunction, of actin and SEC14p defects includes features that are unique to the *sac1* mechanism, and are not shared by the suppression mechanisms operating in the other *sac* mutants we have tested. We assign considerable relevance to the specific inositol auxotrophy exhibited by *sac1* yeast strains not only because this phenotype correlated with suppression of *sec14* defects in the survey of *sac* mutants (Fig. 9), but also because a similar inositol auxotrophy is associated with another suppressor of *sec14* defects. The *bsd2-1* mutation represents a dominant bypass suppressor of *sec14* defects (Cleves et al., 1991*b*). This allele also phenotypically manifests itself in an inositol auxotrophy that is itself a dominant trait (T. P. McGee, and V. A. Bankaitis, unpublished data). The finding that inositol auxotrophy is a phenotype shared by two distinct classes of mutations that suppress *sec14* defects suggests that this inositol auxotrophy is somehow reflective of the mechanism by which *sec14* and actin defects are suppressed in *sac1* strains.

What possible clues might the *sac1*-associated inositol auxotrophy provide with respect to SAC1p function in cells and how SAC1p dysfunction may influence the organization of the actin cytoskeleton and the cellular requirement for SEC14p? As inositol is a direct precursor of the essential glycerophospholipid PI, which itself provides the inositol moiety in the biosynthesis of inositol sphingolipids (Becker and Lester, 1980), the inositol auxotrophy suggests some relationship between SAC1p function and inositol glycerophospholipid metabolism. It may be relevant that the mammalian actin binding proteins profilin, gelsolin and cofilin exhibit a high affinity binding of phosphoinositides in vitro (Goldschmidt-Clermont et al., 1990; Lassing and Lindberg, 1985; Yin et al., 1988; Yonezawa et al., 1991). Pollard and co-workers have obtained some biochemical evidence to support the notion that the cytosolic protein profilin sequesters phosphatidylinositol 4,5-bisphosphate (PIP_2), thus rendering the bound PIP_2 inaccessible to degradation by unstimulated phospholipase C (Goldschmidt-Clermont et al., 1991). These findings suggest a biochemical link between polyphosphoinositides, direct derivatives of the preferred in vitro ligand of the SEC14p (i.e., PI; Daum and Paltauf, 1984), and the regulation of actin assembly.

The notion that SAC1p function somehow interfaces with inositol glycerophospholipids is an attractive one as it suggests a general explanation, within an already familiar conceptual framework, for several of the outstanding phenotypes associated with the loss of SAC1p function (i.e., suppression of *act1-1*^{ts} and *sec14* mutations, a novel inositol auxotrophy, and a dramatic disorganization of the actin cytoskeleton in *sac1* cells challenged with low temperatures). The demonstration that *sac1-26* mutants maintained substantially normal intracellular inositol pools in the face of challenge with inositol-free medium suggests that *sac1* mutants retain wild-type de novo inositol biosynthetic capability (Fig. 10 *A*). Thus, it seems unlikely that the *sac1*-associated inositol auxotrophy is the result of an inositol biosynthetic defect. As the data also failed to indicate an obvious inositol utilization defect in Δ*sac1* mutants (Fig. 10 *B*), it seems most likely that *sac1* mutants require elevated levels of inositol for cell growth. An elevated inositol requirement might reflect some unusual turnover of inositol phospholipids in *sac1* mutants, perhaps due to the loss of some SAC1p-dependent inositol phospholipid sequestration function. The finding that bulk membrane PI levels of Δ*sac1* mutants were indistinguishable from those of wild-type strains, however, does not reveal a wholesale defect in PI metabolism in *sac1* mutants (Fig. 10 *B*). It will be of interest to determine whether *sac1* mutations affect the PI content of yeast Golgi membranes.

The idea that SAC1p functions in inositol phospholipid sequestration has some important ramifications for the genetic (i.e., allele specificity) argument that SAC1p is a candidate actin binding protein. If SAC1p is involved in regulating (i.e., antagonizing) inositol PL turnover in cells, it need not exhibit a physical association with actin in order for loss of SAC1p function to phenotypically manifest itself either in the observed disorganization of the actin cytoskeleton in vivo or in the observed allele-specific genetic interactions with *act1* mutations. For example, loss of SAC1p function might upset the normal function of other actin binding proteins that interact with actin in an inositol phospholipid-sensitive manner; thereby eliciting the observed allele-specific effects on actin cytoskeleton function and organization in cells via an indirect lipid-mediated effect. In this scenario, deregulated inositol PL turnover in *sac1* mutants could suppress actin defects associated with inefficient polymerization of mutant G-actin monomers, yet further exacerbate actin defects associated with inefficient disassembly of mutant F-actin structures. It is interesting to note that *act1-1*^{ts}, a mutation suppressed by *sac1*, has been suggested to encode polymerization-defective actin whereas *act1-2*^{ts}, a mutation that exhibits synthetic lethality with *sac1*, has been proposed to result in the formation of disassembly-defective F-actin structures (Novick et al., 1989). Such a model describes a situation where a remarkable allele specificity might be generated not as a result of altered protein–protein interactions between two mutant polypeptides but, rather, from a more indirect alteration in the regulation of the assembly of one of the mutant polypeptides. Alternatively, if SAC1p itself binds G-actin in an inositol PL-sensitive manner, the various *sac1* effects on the organization of the actin cytoskeleton and the accompanying *sac1–act1* genetic interactions can be accommodated into a model directly analagous to the profilin paradigm as proposed by Goldschmidt-Clermont et al. (1991).

The data presented in this report also offer interesting pos-

sibilities with regard to what SEC14p-dependent biochemical functions might determine the secretory competence of yeast Golgi membranes. Our previous results have suggested that PC synthesis via the CDP-choline pathway is not compatible with Golgi secretory function in vivo, and that the essential role of SEC14p is to moderate the antagonism between these two cellular functions by maintaining an appropriate phospholipid composition in yeast Golgi membranes (Cleves et al, 1991*a*, *b*). One implication of those data is that excess PC is detrimental to Golgi secretory function. The general models for SAC1p function entertained here raise the alternative, but not mutually exclusive, possibility of a SEC14p-dependent involvement of inositol phospholipids, or perhaps the local turnover of such phospholipids, in yeast Golgi secretory function.

V. A. Bankaitis dedicates this work to the memory of his friend and mentor, Philip J. Bassford, Jr. We wish to thank Beth Jones, Bob Fuller, Brian Haarer, David Drubin, Peter Novick, Alison Adams, and A. Tzagaloff for antisera, plasmids, and yeast strains, P. Novick and George Carman for helpful discussions, and D. Drubin, Barclay Browne, and two anonymous reviewers for critical comments on the manuscript. We are particularly grateful to Dr. Michael Friedlander (Neurobiology Research Center, University of Alabama at Birmingham) for providing us access to the luminometer.

This work was supported by Public Health Service Grant GM-44530 from the National Institutes of Health (to V. A. Bankaitis).

Received for publication 8 March 1993, and in revised form 19 April 1993.

References

Adams, A. E. M., and J. R. Pringle. 1984. Relationship of actin and tubulin distribution to bud growth in wild-type and morphogenetic-mutant *Saccharomyces cerevisiae*. *J. Cell Biol.* 98:934–945.

Adams, A. E. M., D. Botstein, and D. G. Drubin. 1989. A yeast actin-binding protein is encoded by *SAC6*, a gene found by suppression of an actin mutation. *Science (Wash. DC).* 243:231–233.

Ames, B. N. 1966. Assay of inorganic phosphate, total phosphate and phosphatases. *Methods Enzymol.* 8:115–116.

Atkinson, K. D. 1984. *Saccharomyces cerevisiae* recessive suppressor that circumvents phosphatidylserine deficiency. *Genetics.* 108:533–543.

Bankaitis, V. A., D. E. Malehorn, S. D. Emr, and R. Greene. 1989. The *Saccharomyces cerevisiae SEC14* gene encodes a cytosolic factor that is required for transport of secretory proteins from the yeast Golgi complex. *J. Cell Biol.* 108:1271–1281.

Bankaitis, V. A., J. R. Aitken, A. E. Cleves, and W. Dowhan. 1990. An essential role for a phospholipid transfer protein in yeast Golgi function. *Nature (Lond.).* 347:561–562.

Becker, G. W., and R. L. Lester. 1980. Biosynthesis of phosphoinositol-containing sphingolipids from phosphatidylinositol by a membrane preparation from *Saccharomyces cerevisiae*. *J. Bacteriol.* 142:747–754.

Bolivar, F., R. L. Rodriguez, P. J. Greene, M. C. Betlach, H. L. Heynecker, H. W. Boyer, J. H. Crosa, and S. Falkow. 1977. Construction and characterization of new cloning vehicles. II. A multipurpose cloning system. *Gene.* 2:95–113.

Bowser, R., and P. Novick. 1991. Sec15 protein, an essential component of the exocytic apparatus, is associated with the plasma membrane and with a soluble 19.5S particle. *J. Cell Biol.* 112:1117–1131.

Carman, G. M., and S. A. Henry. 1989. Phospholipid biosynthesis in yeast. *Annu. Rev. Biochem.* 58:635–669.

Casadaban, M. J., and S. N. Cohen. 1980. Analysis of gene control signals by DNA fusion and cloning in *Escherichia coli*. *J. Mol. Biol.* 138:179–207.

Christie, W. W. 1987. Chromatographic and spectroscopic analysis of lipids. *In* Lipid Analysis (second edition). W. W. Christie, editor. Pergamon Press, Oxford, Great Britain. 34–38.

Cleves, A. E., P. J. Novick, and V. A. Bankaitis. 1989. Mutations in the *SAC1* gene suppress defects in yeast Golgi and yeast actin function. *J. Cell Biol.* 109:2939–2950.

Cleves, A. E., T. P. McGee, and V. A. Bankaitis. 1991*a*. Phospholipid transfer proteins: a biological debut. *Trends Cell Biol.* 1:30–34.

Cleves, A. E., T. P. McGee, E. A. Whitters, K. M. Champion, J. R. Aitken, W. Dowhan, M. Goebl, and V. A. Bankaitis. 1991*b*. Mutations in the CDP-choline pathway for phospholipid biosynthesis bypass the requirement for an essential phospholipid transfer protein. *Cell.* 64:789–800.

Daum, G., and F. Paltauf. 1984. Isolation and characterization of a phospholipid transfer protein from yeast cytosol. *Biochim. Biophys. Acta.* 794: 385–391.

Donahue, T. F., and S. A. Henry. 1981. *Genetics.* 98:491–503.

Dunn, T. M., and D. Shortle. 1990. Null alleles of *SAC7* suppress temperature-sensitive actin mutations in *Saccharomyces cerevisiae*. *Mol. Cell. Biol.* 10: 2308–2314.

Franzusoff, A., and R. Schekman. 1989. Functional compartments of the yeast Golgi apparatus are defined by the *sec7* mutation. *EMBO (Eur. Mol. Biol. Organ.) J.* 8:2695–2702.

Franzusoff, A., K. Redding, J. Crosby, R. S. Fuller, and R. Schekman. 1991. Localization of components involved in protein transport and processing through the yeast Golgi apparatus. *J. Cell Biol.* 112:27–37.

Fugiki, Y., A. L. Hubbard, S. Fowler, and P. B. Lazarow. 1982. Isolation of intracellular membranes by means of sodium carbonate treatment: application to endoplasmic reticulum. *J. Cell Biol.* 93:97–102.

Goldschmidt-Clermont, P. J., L. M. Machesky, J. J. Baldassare, and T. D. Pollard. 1990. The actin-binding protein profilin binds to PIP_2 and inhibits its hydrolysis by phospholipase C. *Science (Wash. DC).* 247:1575–1578.

Goldschmidt-Clermont, P. J., J. W. Kim, L. M. Machesky, S. G. Rhee, and T. D. Pollard. 1991. Regulation of phospholipase C-γ1 by profilin and tyrosine phosphorylation. *Science (Wash. DC).* 251:1231–1233.

Greer, C., and R. Schekman. 1982. Actin from *Saccharomyces cerevisiae*. *Mol. Cell. Biol.* 2:1270–1278.

Gudermann, T. W., and T. G. Cooper. 1986. A sensitive bioluminescence assay for *myo*-inositol. *Anal. Biochem.* 158:59–63.

Hanahan, D. 1983. Studies on transformation of *Escherichia coli* with plasmids. *J. Mol. Biol.* 166:557–580.

Hoshizaki, D. K., J. E. Hill, and S. A. Henry. 1990. The *Saccharomyces cerevisiae INO4* gene encodes a small, highly basic protein required for derepression of phospholipid biosynthetic enzymes. *J. Biol. Chem.* 265: 4736–4745.

Ito, H., Y. Fukuda, K. Murata, and A. Kimura. 1983. Transformation of intact yeast cells treated with alkaline cations. *J. Bacteriol.* 153:163–168.

Kaiser, C., and R. Schekman. 1990. Distinct set of *SEC* genes govern transport vesicle formation and fusion early in the secretory pathway. *Cell.* 61: 723–733.

Kennett, R. H., T. J. McKeon, and K. B. Bechtol, editors. 1980. Monoclonal Antibodies. Plenum Publications, NY. 139–302.

Kleid, D. G., D. Yansura, B. Small, D. Dowbenko, D. M. Moore, M. J. Grubman, P. D. McKercher, D. O. Morgan, B. H. Robertson, and H. L. Bachrach. 1981. Cloned viral protein vaccine for foot-and-mouth disease: responses in cattle and swine. *Science (Wash. DC).* 214:1125–1129.

Klig, L. S., M. J. Homann, G. M. Carman, and S. A. Henry. 1985. Coordinate regulation of phospholipid biosynthesis in *Saccharomyces cerevisiae*: Pleiotropically constitutive *opi1* mutant. *J. Bacteriol.* 162:1135–1141.

Klionsky, D. J., L. M. Banta, and S. D. Emr. 1988. Intracellular sorting and processing of a yeast vacuolar hydrolase: Proteinase A propeptide contains vacuolar targeting information. *Mol. Cell Biol.* 8:2105–2116.

Laemmli, U. K. 1970. Cleavage of structural proteins during the assembly of the head of bacteriophage T4. *Nature (Lond.).* 227:680–685.

Maniatis, T., E. F. Fritsch, and J. Sambrook. 1982. Molecular Cloning: A Laboratory Manual. Cold Spring Harbor Laboratory, Cold Spring Harbor, N.Y.

Nikoloff, D. M., P. McGraw, and S. A. Henry. 1992. The INO2 gene of Saccharomyces cerevisiae encodes a helix-loop-helix protein that is required for activation of phospholipid biosynthesis. *Nucleic Acids Research.* 20: 3253–3253.

Novick, P., C. Field, and R. Schekman. 1980. Identification of 23 complementation groups required for post-translational events in the yeast secretory pathway. *Cell.* 21:205–215.

Novick, P., B. C. Osmond, and D. D. Botstein. 1989. Suppressors of yeast actin mutations. *Genetics.* 121:659–674.

Pringle, J., R. Preston, A. Adams, T. Stearns, D. Drubin, B. Haarer, and E. Jones. 1989. Fluorescence microscopy methods for yeast. *Meth. Cell Biol.* 31:357–435.

Redding, K., C. Holcomb, and R. S. Fuller. 1991. Immunolocalization of KEX2 protease identifies a putative late Golgi compartment in the yeast *Saccharomyces cerevisiae*. *J. Cell Biol.* 113:527–538.

Rose, M. D., L. M. Misra, and J. P. Vogel. 1989. KAR2, a karyogamy gene, is the yeast homolog of the mammalian BiP/GRP78 gene. *Cell.* 57: 1211–1221.

Rothstein, R. J. 1983. One-step gene disruption in yeast. *Methods Enzymol.* 101:202–211.

Salama, S. R., A. E. Cleves, D. E. Malehorn, E. A. Whitters, and V. A. Bankaitis. 1990. Cloning and characterization of *Kluyveromyces lactis SEC14*, a gene whose product stimulates Golgi secretory function in *Saccharomyces cerevisiae*. *J. Bacteriol.* 172:4510–4521.

Sherman, F., G. R. Fink, and J. B. Hicks. 1983. Methods in Yeast Genetics. Cold Spring Harbor Laboratory, Cold Spring Harbor, NY.

Silhavy, T. J., M. L. Berman, and L. W. Enquist, editors. 1984. Experiments with Gene Fusions. Cold Spring Harbor Laboratory, Cold Spring Harbor, NY. 137–183.

Yin, H. L., K. Iida, and P. A. Janmey. 1988. Identification of a polyphosphoinositide-modulated domain in gelsolin which binds to the sides of actin filaments. *J. Cell Biol.* 106:805–812.

Yonezawa, N., Y. Homma, I. Yahara, H. Sakai, and E. Nishida. 1991. A short sequence responsible for both phosphoinositide binding and actin binding activities of cofilin. *J. Biol. Chem.* 266:17218–17221.